Published November 27, 2019

Cryoturbation and Carbon Stocks in Gelisols under Late-Successional Black Spruce Forests of the Copper River Basin, Alaska

Nicolas A. Jelinski*
Michael J. Sousa
Dep. of Soil, Water and Climate
Univ. of Minnesota Twin-Cities
1991 Upper Buford Circle
Saint Paul, MN 55108

Andrea Williams
USDA–NRCS
4850 Miller Trunk Highway, Suite 1B
Duluth, MN, 55811

Edward GreyBear
Ahtna, Inc.
115 Richardson Hwy
Glennallen, AK, 99588
and
Ahtna Intertribal Resource Commission
Mile 187 Glenn Highway
Glennallen, AK 99588
and
Univ. of Alaska-Fairbanks
900 Yukon Drive
Fairbanks, AK 99775

Katie Finnesand
Ahtna, Inc.
115 Richardson Hwy
Glennallen, AK, 99588

Dennis Mulligan
Cory Cole
USDA–NRCS
800 East Palmer-Wasilla Hwy., Suite 100
Palmer, AK 99645

Michele D. Stillinger
Dougherty Family College
Univ. of St. Thomas
1000 LaSalle Ave
Minneapolis, MN 55403

Joshua M. Feinberg
Dep. of Earth and Environmental Sciences–Institute for Rock Magnetism
Univ. of Minnesota Twin-Cities
116 Church St SE
Minneapolis, MN 55455

In the Alaskan discontinuous permafrost zone, soils developed under black spruce [*Picea mariana* (Mill.) Britton, Sterns & Poggenb.] forests are affected by fire over return intervals ranging from decades to centuries and cycle between recently burned and late-successional stages. Soils under late-successional forests therefore provide foundational information regarding the potential recovery of soil and permafrost characteristics following disturbance by fire. Twenty-two permafrost-affected soils (predominantly Histoturbels with minor components of Sapristels and Aquiturbels) were investigated under late-successional black spruce in the Copper River Basin, which contains the largest expanse of glaciolacustrine sediments in Alaska. Although these soils are well insulated (organic layer thicknesses of 31 ± 10 cm) and fine-textured with a relatively shallow permafrost table (69 ± 19 cm), 87% of the 129 described mineral soil horizons across these sites showed morphological evidence of cryoturbation. Depth trends in water content and bulk density were consistent with an ice-rich upper permafrost, with suspended cryostructures most common in the upper permafrost. Soil organic carbon (SOC) stocks to 1 m averaged 46 ± 12 kg m^{-2}, with 44% of the SOC stocks contained in cryoturbated mineral horizons, many of which were identified well below the current permafrost table. The most likely mechanism of cryoturbation in these soils is post-fire active layer deepening followed by solutioning and diapirism, generating SOC stocks in cryoturbated mineral materials of the upper permafrost. Future changes in climate or fire frequency that affect active layer depth may therefore have the potential to affect cryoturbation processes and carbon stocks in these soils.

Abbreviations: AICc, corrected Akaike's information criterion; BIC, Bayesian information criterion; CRB, Copper River Basin; LOI, loss on ignition; OLT, organic layer thickness; SIC, soil inorganic carbon; SIPRE, US Snow, Ice and Permafrost Research Establishment; SOC, soil organic carbon; TC, total carbon; TN, total nitrogen.

Soils of permafrost regions are globally important mediators of ecosystem physical, chemical, and biological processes and large reservoirs of terrestrial organic carbon (C) (Grosse et al., 2016; Hugelius et al., 2014; Ping

Core Ideas

- **Eighty-seven percent of mineral soil materials showed evidence of cryoturbation.**
- **Soil organic C stocks were evenly partitioned between organic materials and cryoturbated mineral materials.**
- **Organic C stocks on lacustrine sediments under black spruce averaged 46 kg C m^{-2}.**
- **Post-fire solutioning and diapirism may be two likely mechanisms of cryoturbation in these soils.**

Soil Sci. Soc. Am. J. 83:1760–1778
doi:10.2136/sssaj2019.07.0212
Received 8 July 2019.
Accepted 24 Sept. 2019.
*Corresponding author (jeli0026@umn.edu).

et al., 2015). In the discontinuous permafrost zone, active layer and permafrost dynamics are spatially and temporally dynamic and are dependent on a wide range of environmental factors (Jorgenson et al., 2010). Because ecosystem-scale environmental change is occurring rapidly in the discontinuous permafrost zone in Alaska (Pastick et al., 2017), it is important to understand the current state and properties of these soils so that future changes can be better predicted and monitored (Mishra et al., 2013).

In Alaska, most of the permafrost-affected soils in the discontinuous permafrost zone lie in the Alaskan interior, the Yukon-Kuskokwim Delta, and the Copper River Basin (CRB) (Gallant et al., 1995; Jorgenson et al., 2008; Nowacki et al., 2001) physiographic regions. With the exception of the Yukon-Kuskokwim Delta, a significant proportion of these soils occurs under boreal forest vegetation that is dominated or co-dominated by black spruce [*Picea mariana* (Mill.) Britton, Sterns & Poggenb] (LANDFIRE, 2017), accounting for 36 to 44% of the land area in the Alaskan interior and ~38% of the land area in the CRB (Chapin et al., 2006; Gallant et al., 1995; LANDFIRE, 2017; Yarie and Billings, 2002).

To date, most of the permafrost-affected soils under black spruce investigated in Alaska have been in the Alaskan interior (Hollingsworth, 2004; O'Donnell, 2010; Viereck et al., 1986); comparatively little data are available on soils from the CRB (Ping et al., 2010). Although the parent materials for permafrost-affected soils in the Alaskan interior are dominated by loess, alluvium, and/or residuum (Ping et al., 2004), the CRB is home to the largest expanse of glaciolacustrine sediments in Alaska. Numerous pro-glacial lakes formed in the intermontane basin of the Copper River, depositing sediment packages from ~58,000 to ~10,000 yBP (Bennett et al., 2012; Ferrians, 1984; Rubin and Alexander, 1960), which were subsequently exposed after the early Holocene drainage of Glacial Lake Ahtna (Wiedmer et al., 2010; Williams and Galloway, 1986). Permafrost-affected soils that formed under black spruce on glaciolacustrine sediments dominate the flat, poorly drained landscape of the central CRB and are characterized by high clay contents, thick organic materials, and poor drainage (Clark and Kautz, 1999). The physiographic context and soil-forming factors at work in the CRB are therefore different from those of loessial soils in the Alaskan interior (Ping et al., 2004).

Cryoturbation and near-surface permafrost properties play an important role in the determination of C distributions and the stabilization and accumulation of C with depth in permafrost-affected soils (Bockheim, 2007; Ping et al., 2015). Previous work suggests that cryoturbation activity (observed through morphological evidence of the sequestration of C-rich materials into the subsoil or near the permafrost table) should be reduced in permafrost-affected soils of the CRB due to thick insulating organic layers (Reiger, 1983) and the lower frost susceptibility of clayey lacustrine materials relative to the silt-rich loessial soils of the Alaskan interior (Ping et al., 2004). This has been supported by recent regional meta-analyses (Palmtag and Kuhry, 2018) and by data from engineering studies on the effects of particle size on the frost susceptibility of sediments (Carter and Bentley, 1991).

Despite physical factors that would seem to inhibit the dynamic processes necessary for widespread cryoturbation to occur in the CRB, fire is an ecosystem process that could contribute to fluctuating active layer thickness and cryoturbation activity over long timescales (Koven et al., 2009). Black spruce–dominated forests are "born to burn" (Chapin et al., 2006), and all soils formed under black spruce are sensitive to fire disturbances due to potential organic layer removal and near-surface permafrost degradation, depending on fire severity (Houle et al., 2018; Minsley et al., 2016). Estimated mean fire return intervals across Alaska range from <30 to >500 yr (Fryer, 2014). Holocene fire frequencies in the CRB tend to be lower than those for interior Alaska (mean estimated return intervals of >500 yr before 3800 yBP and 150 yr after 2000 yBP) (Fryer, 2014; Lynch et al., 2004). Although documented records of historical fires in the CRB tend to show an increase in fire frequency in the CRB due to human activities during the late 1800s and early 1900s (Alaska Land Use Council, 1984), fires since 1940 have been relatively infrequent in the CRB relative to those in the interior (Alaska Interagency Coordination Center, 2018). Thus, all black spruce sites in the CRB are at some stage of post-fire succession.

The goal of this study was to collect foundational data that would reflect predominantly environmental controls (avoiding differing times because fire disturbance is a confounding variable) on soil characteristics, soil C stocks, and soil C partitioning under black spruce in the CRB with a focus on late-successional black spruce stands that represent relatively stable end points to successional trajectories (Johnstone et al., 2008). The objectives of this work were therefore to characterize the (i) morphology, (ii) near-surface cryostructures, (iii) C partitioning, and (iv) C stocks in soils under late-successional black spruce stands formed in lacustrine sediments in the CRB. This foundational information is critical for understanding the widespread ecological implications of future environmental change in permafrost-affected soils (Pastick et al., 2015, 2017, 2019).

MATERIALS AND METHODS

Landscape Context and General Properties of Soils Under Late-Successional Black Spruce in the Copper River Basin

Soils under late-successional black spruce in the glaciolacustrine uplands of the CRB are of large extent and form the major part of an ecological gradient across the landscape from moderately well-drained soils with low permafrost table that are typically on degraded palsas or lithalsas (Vasil'chuk et al., 2015), dominated by aspen (*Populus tremuloides* Michx.) and white spruce [*Picea glauca* (Moench) Voss] (Supplemental Fig. S1), to treeless, very poorly drained depressional wetland sites under sedge (*Carex* sp.) (Supplemental Fig. S1; Supplemental Table S1). The entire CRB landscape has experienced fire at return intervals on the order of centuries (Fryer, 2014; Lynch et al., 2004). Soils under late-successional stands of black spruce are typically very poorly drained, whereas early- to mid-successional stands of mixed black and white spruce tend to show better drainage characteristics due to

a lowering of the permafrost table associated with a reduction in thickness of the insulating organic layer post-fire (Supplemental Fig. S1; Supplemental Table S1). These soils are formed predominantly in lacustrine sediments, with a thin, discontinuous loess cap that increases rapidly in thickness toward the narrow valley of the Copper River in the southernmost outlet of the basin (Muhs et al., 2013). Near-surface pH increases in burned sites from the contribution of cation-rich ash to the organic layer (Supplemental Table S1). This process increases rates of decomposition and can result in suppression of organic layer recovery in burned areas on timescales of decades to centuries (Clark and Kautz, 1999).

Mineralogy in the fine sand and very fine sand fractions suggests that glass content in the thin, discontinuous loess and degraded organic materials (9 and 11% in fine sand and very fine sand fractions, respectively) is significantly higher than that found in lacustrine sediments (2 and 3% in fine sand and very fine sand fractions, respectively) (Supplemental Table S2). These numbers are broadly consistent with sparse data available from a previous soil survey in the southern CRB (4% glass in the coarse silt and ~15% glass in the very fine sand fraction of a loess cap over lacustrine materials). Although glass content is generally >5% in loess and organic materials in the study area (Supplemental Table S2), these materials do not meet andic criteria due to low P retention (<63% in all samples) and low ammonium oxalate–extractable Al and Fe (<1% in all samples) (Soil Survey Staff, 2014a). The increase in glass content but the absence of defined ash layers suggests minor deposition from localized volcanic activity over the last millennia, perhaps from the Hayes volcano or others along the Cook Inlet (Riehle et al., 1990). Although closer in proximity to the CRB, it is unlikely that Mt. Churchill (the source of the extensive White River ash in eastern Alaska and the Yukon) would be a plausible source given reconstructions of ash lobe distributions (Lerbekmo, 2008; Preece et al., 2014). Chlorite, montmorillionite, and micaceous minerals (e.g., biotite, muscovite, and phlogopite) are the dominant phyllosilicates present in the clay fraction of CRB glaciolacustrine sediments (Clark and Kautz, 1999).

Site Selection, Soil Sampling, and Sample Preparation

In late August 2017 (close to the timing of maximum thaw depth) (Dyrness, 1982), soils across 22 late-successional black spruce sites on glaciolacustrine sediments in the central CRB near Gakona, AK (located in three different site clusters) were investigated based on accessibility and lack of obvious evidence of recent fire disturbance (Fig. 1). The soils and landscapes sampled as a part of this project are part of the Native Territory of the Ahtna people.

Although the entire CRB landscape has experienced fire at some time in the past, achieving the goals of this study required the selection of sites that were most likely to represent late-successional, mature black spruce stands. This was determined by a visual estimation of tree stand age and structure (mixed-age stands), by satellite imagery, and by a lack of standing dead or live trees that showed evidence of previous fire disturbance, such as scars or charcoal on their bark. Field observations were then confirmed by tree ring counts in cores; the age ranges of the trees in several plots are reported in Supplemental Table S1. We made a concerted effort to select only late-successional black spruce sites for this study; however, even late-successional black spruce sites may be a reflection of both site environmental characteristics and past fire legacies that can influence successional trajectories (Hollingsworth, 2004; Hollingsworth et al., 2006).

At each site, a soil pit (~60 cm × 60 cm) was excavated to the bottom of the active layer following standard procedures for sampling permafrost-affected soils (Ping et al., 2013). Sampling of frozen material below the active layer was accomplished through the use of a US Snow, Ice and Permafrost Research Establishment (SIPRE) corer (Rand and Mellor, 1985). Depending on the depth of frozen materials, a combination of the soil pit and a core or set of cores was used to observe material to at least 100 cm in depth at each of the sites. At one site, refusal of the SIPRE corer due to large coarse fragments (likely dropstones) limited observations to a depth of 78 cm (Sites 1–4) (Supplemental Table S3). Active-layer morphology was described in the field, and morphological properties, including soil color, soil structure, soil texture, visible secondary carbonates, and visual differences in volume estimates of coarse fragments, were used to define genetic horizons (Schoeneberger et al., 2012). For horizons demonstrating morphological evidence of cryoturbation (such as the presence of both mineral materials low in organic C and materials rich in organic C), the volume percentage of each of the components of the horizon was estimated in the field using percent cover diagrams provided in the *Field Book for Describing and Sampling Soils* version 3.0 (Schoeneberger et al., 2012).

For frozen materials extracted by SIPRE corer, morphology was described in the field using horizon nomenclature (Schoeneberger et al., 2012), morphological properties (Schoeneberger et al., 2012), and cryostructure descriptions following Ping et al. (2008) and French and Shur (2010). Note that cryogenic soil structure (soil structural units caused primarily by ice segregation and/or freeze thaw processes) (Ping et al., 2008) is different from cryostructure (ice structure reflecting the amount, orientation, arrangement, and distribution of pore and segregated ice within frozen materials) (French and Shur, 2010). In this manuscript, cryogenic soil structures (i.e., soil structure) were described in the active layer, whereas cryostructures were described in the upper permafrost. Morphological evidence was used to estimate the depth to the bottom of the transient layer (i.e., the uppermost portion of the transition zone that includes both the transient and intermediate layers), which is the portion of the upper permafrost that may join the active layer over decadal timescales due to environmental fluctuations (French and Shur, 2010; Shur et al., 2005). This was estimated by the first appearance of ice-rich materials that are characteristic of the bottom of the transient layer, such as suspended (ataxitic) cryostructures (Murton and French, 1994) or ice lenses (Shur et al., 2005).

Frozen cores were segmented using a 12V Craftsman multitool and placed in Ziploc bags to prevent water loss. All samples were weighed in bags within 8 h of sampling (subtracting the mass of bags) to record the field moist mass. Across all 22 sites, a total of 220 physical samples were collected.

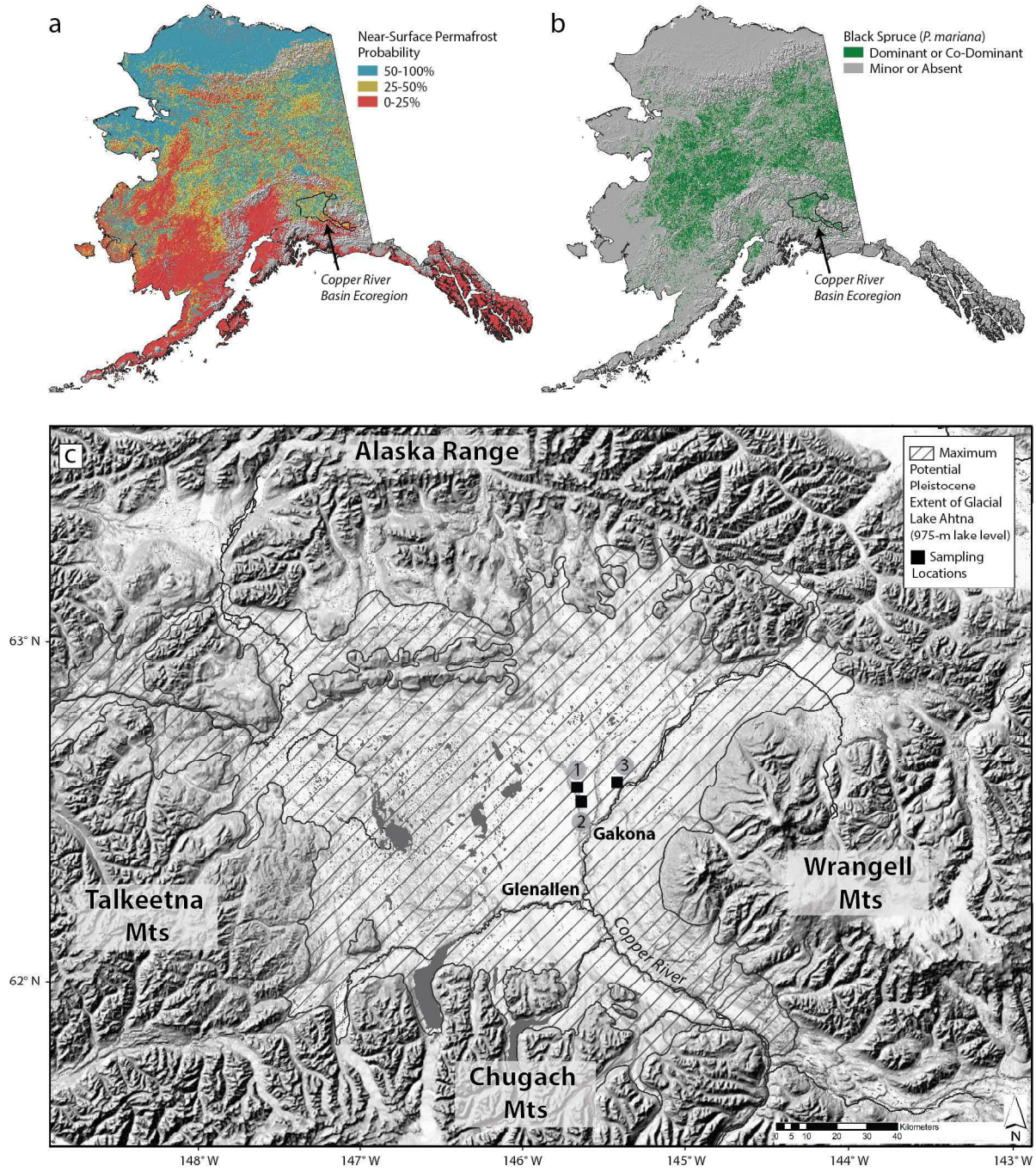

Fig. 1. Location of sampling sites in state and regional context. The location of the Copper River Basin (CRB) physiographic region in relationship to (a) near-surface (<1 m) permafrost probability in Alaska (adapted from Pastick et al., 2015) and (b) forested areas in Alaska where *Picea mariana* (black spruce) is a dominant or codominant tree species (LANDFIRE, 2017). (c) Location of sampling sites in the CRB physiographic region in relation to the 975-m lake level of Glacial Lake Ahtna (adapted from Wiedmer et al., 2010) and locations of sampling sites (*n* = 22) within three major sampling clusters (Cluster 1, *n* = 8; Cluster 2, *n* = 8; Cluster 3, *n* = 6). The extent of the CRB physiographic region largely follows the boundaries of the maximum extent of Glacial Lake Ahtna, with the exception of the northwestern area intruding into the Talkeetna Mountains.

Samples were shipped to the University of Minnesota, where they were dried at 60°C, hand pulverized, and sieved to separate the fine earth (<2 mm) from the coarse fragments (>2 mm). The fine earth fraction (<2 mm) was used for characterization of soil pH, soil organic C (SOC), soil inorganic C (SIC), particle size distribution, and loss on ignition (LOI). Particles (typically fine gravels) that were >2 mm were retained, shaken overnight in deionized water to remove adhering soil particles, oven dried for 24 h at 105°C, and weighed. Coarse fragments present in the samples were typically fine gravels and accounted for, on average, <2% of the bulk mass of the sample collected in the field. On the same day that physical and chemical characterization of fine earth (<2 mm) was initiated, a subsample of the air-dried material was placed in a drying oven for 24 h at 105°C and weighed before and after drying to account for the moisture content of the air-dried sample used for analysis. Thus, the bulk densities reported, and all other proportions of

soil constituents reported in the data, represent percentages of oven-dried fine-earth (<2 mm) material.

Sample Characterization: pH, Particle Size Distribution, Soil Carbon, Gravimetric Water Content, and Bulk Density

Soil pH for mineral samples was determined in 1:1 slurry of 5 g of air-dried soil and 5 mL of water (pH_{H2O}) followed by addition of 5 mL of 0.01 M $CaCl_2$ (pH_{CaCl2}) (Soil Survey Staff, 2014a). For organic soil samples, a 2:1 soil/water slurry was used because a 1:1 slurry for organics did not typically produce enough free water once added to dry organics to produce a reliable slurry and pH measurement.

Total C (TC, g 100 g^{-1}) in soil and total nitrogen (TN, g 100 g^{-1}) were determined on a subset of samples by dry combustion at 800°C using a LECO 2000 CN analyzer. For mineral samples with a pH >5.5, SIC was determined by acid fumigation in a desiccator using concentrated HCl for 8 h (Harris et al., 2001). The TC of unfumigated samples was subtracted from the TC for fumigated samples to arrive at SIC concentrations (g 100 g^{-1}) and SOC concentrations (g 100 g^{-1}). All samples were analyzed for LOI (weight %) at 550°C for 5 h, and predicted SOC was determined by linear regression of dry combustion TC results on LOI for a subset of samples (SOC = 0.538 × LOI − 0.816; $R^2 = 0.994$; $p < 0.001$; $n = 136$). The combustion temperature and duration chosen for LOI measurements were selected as a compromise between other previous LOI methodologies used for permafrost-affected soils (550°C for 6 h) (Hugelius et al., 2012), recommendations from methodological comparisons (550°C for 3 h) (Hoogsteen et al., 2015), and studies involving LOI from soils containing measurable carbonates (550°C for 4 h) (McCray et al., 2012; Wright et al., 2008).

Mineral soil texture was determined by laser particle size analysis, with quality control samples determined by the pipette and hydrometer methods (Grigal, 1973; Soil Survey Staff, 2014a). Samples for particle size analysis were air dried, passed through a 2-mm sieve, and hand homogenized prior to subsampling. Three 0.5-g subsamples were then obtained and dispersed overnight in 200 mL of deionized H_2O with Na-hexametaphosphate (5 mL) and Na-hypochlorite (5 mL) prior to standard analysis on a Malvern Mastersizer 3000. The refractive indices of soil and the water-based dispersant were assumed to be 1.549 and 1.33, respectively (Miller and Schaetzl, 2012). Extensive in-house validation was conducted on known size fractions of sand, silt, and clay to optimize laser particle size data for comparison with the more traditional hydrometer method. Based on this in-house compilation, the clay–silt break was set at 8 mm, which is consistent with other studies (Konert and Vandenberghe, 1997). To eliminate bias due to small subsample sizes, triplicate analyses of each of the three subsamples were conducted and compared. The set of three that was most different from the other (two) subsamples was discarded. The two most comparable triplicate sets were used to calculate the mean particle size distribution ($n = 6$) for use in subsequent analyses.

Bulk density samples were collected using standardized methodologies, depending on thermal state and material type (Ping et al., 2013). Because it is inappropriate to use the clod or ring methods on organic materials, surface organic horizon bulk densities were collected using a serrated knife to cut blocks of 262 cm^3 (2 in. × 2 in. × 4 in.) from the pit face. For horizons that were too thin to be sampled using this standardized size, blocks were cut, and dimensions were measured to the nearest centimeter to determine volume in the field. Unfrozen mineral soil samples were collected using the ring method, attached to a short slide hammer. For unfrozen mineral or cryoturbated horizons, bulk density samples were collected from the pit face using a core of known volume and sharp beveled edges. For frozen materials, a SIPRE corer (7.6 cm inner diameter) was used to recover cylindrical samples, which were subsequently segmented following description of the core. All frozen samples were quickly sealed in plastic bags to prevent water loss (Michaelson et al., 1996; Ping et al., 2013).

Gravimetric water content (θ_g) for each sample was determined by the difference between the field moist mass of the bulk sample (weighed within 8 h of collection in the field) and the oven dry mass of the bulk sample (obtained by applying a moisture correction to the bulk mass of the air-dried samples after drying a subsample at 105°C for 24 h). Volumetric water content (θ_v) for unfrozen samples was obtained by multiplying θ_g by the bulk density, assuming the density of liquid water to be 1 g cm^{-3}. For frozen samples, θ_v was determined in the same way, except the lower density of ice compared with liquid water was taken into account (0.917 g cm^{-3}) (Weast, 1981).

Statistical Analysis

All statistical analyses were performed in R version 3.3.1 (R Core Team, 2016). The relationship between measured variables was explored in several cases to develop predictive functions. The purpose of developing these functions was to understand the relationship between variables, and therefore if the relationship between two variables was nonlinear we chose not to transform the original data but rather to fit a nonlinear model by evaluating a specific suite of potential nonlinear models commonly used in agricultural and natural resource applications (Archontoulis and Miguez, 2015). A single nonlinear model representing the relationship between two variables was selected from this potential suite of models by evaluating the bias-corrected Akaike's Information Criterion (AICc) and the Bayesian information criterion (BIC) (Akaike, 1998; Schwarz, 1978; Spiess and Neumeyer, 2010) for each potential nonlinear model. The model that minimized AICc and BIC was selected as the final model presented. Values of AICc and BIC are not absolute; rather, they were conditional on the variables under investigation. Therefore, these values are not reported when the nonlinear models are presented in the figures. In all of these cases, a linear model and a null model representing the mean of the dependent variable were evaluated to ensure that a nonlinear model was not unnecessarily over-complex. In cases where a linear model was an appropriate fit, the linear model was selected as the final model presented.

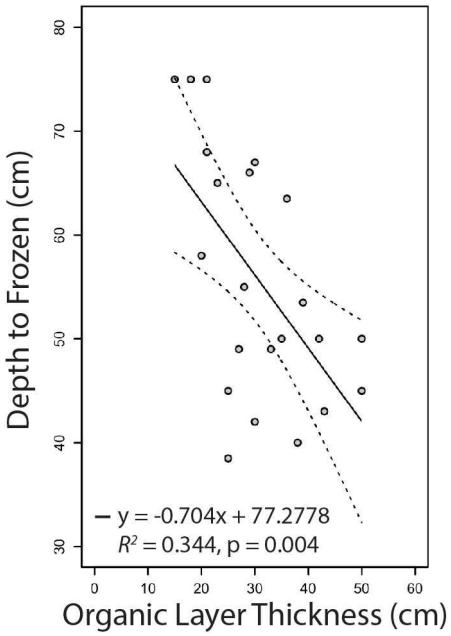

Fig. 2. Relationship between organic layer thickness and observed depth to frozen materials at the time of sampling across all 22 investigated sites under late-successional black spruce in the Copper River Basin, AK. The dotted lines represent the 95% confidence interval around the slope of the linear regression line.

Post hoc analyses for significant differences in response variables between groups after one-way ANOVAs were conducted using Tukey's HSD on group means. Unless otherwise mentioned, all reported uncertainties represent a single standard deviation around the mean. Because samples were collected on the basis of genetic horizons described in the field, the weighted averages of all available soil properties by depth increment were calculated for each sampling site using the "slab" function in the AQP package in R (Beaudette et al., 2013; R Core Team, 2016). Standardized depth-increment weighted averages were used to visualize the relationship between soil properties and depth.

RESULTS

Soil Morphology, Horizon Nomenclature, pH, Texture, and Classification

Across all 22 sites, 206 distinct morphological horizons were described in the field, with a total of 220 physical samples collected due to replicate or component samples from some horizons. Due to the difficulty of assigning some highly organic mineral materials to either organic or mineral materials in the field, 20 morphological horizons were described as transitional in the field (as either OA or AO horizons). Of those 20 transitional horizons, after laboratory analysis of SOC and particle size distributions, 16 were renamed as Oa, and four were renamed as A. Eight horizons were assigned an A master designation in the field, seven of which were renamed to Oa following laboratory data. Among all 206 named and described horizons following final nomenclature reassignment, 7 (3%) were assigned to A horizons, 99 (48%) were assigned to unfrozen and frozen cryoturbated horizons (A/Cjj or C/Ajj), 18 (9%) were assigned to noncryoturbated mineral horizons (C), 42 (20%) were assigned to Oa, 14 (7%) were assigned to Oe, and 26 (13%) were assigned to Oi.

Observed depth to frozen materials at the time of sampling ranged from 39 to 75 cm across all sites (mean, 56 ± 12 cm), and interpreted depth to the bottom of the transient layer ranged from 47 to 124 cm (mean, 69 ± 19 cm) (Supplemental Table S3). Organic layer thickness (OLT) (following reassignment after laboratory analysis for transitional horizons) ranged from 18 to 50 cm (mean, 31 ± 10 cm) (Supplemental Table S3). The OLT was negatively correlated to the depth to frozen materials at the time of sampling (Fig. 2) but varied significantly across sites (R^2 = 0.34; p = 0.004) (Fig. 2). Attempts at multiple linear regression did not find any other site or soil factors that were significant after OLT was included in the model. The relationship between OLT and the depth to the bottom of the transient layer was not significant.

Cryogenic soil structures (structures formed from ice segregation of soil aggregates) in the active layer were observed in all investigated soils throughout the lower active layer and were

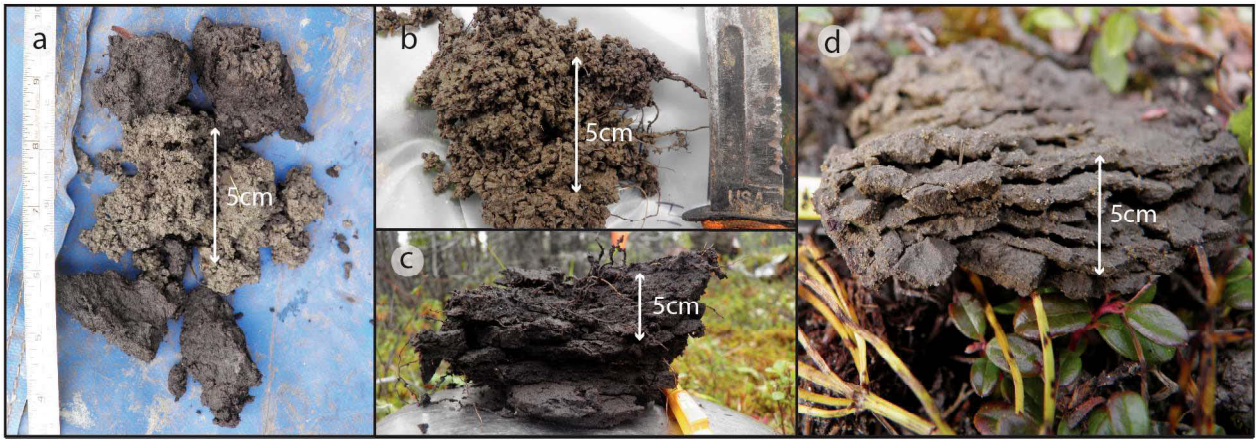

Fig. 3. Cryogenic soil structures observed in the active layer under late-successional black spruce in the Copper River Basin, AK. (a) Example of contrasting cryogenic soil structures in active layer materials; A horizons (top and bottom of image): moderate coarse subangular blocky; C horizons in lacustrine material (center of image): strong very fine to fine angular blocky structure (Sites 2–5). (b) Strong very fine to fine angular blocky cryogenic soil structure in the lower active layer (Sites 1–4). (c) Moderate to strong very thick platy structure in an A horizon (Sites 3 and 4). (d) Strong medium to thick platy structure remains after ice lenses melt out of a frozen sample following removal of a core from the lower active layer (Sites 1 and 2).

highly dependent on material type (Fig. 3a–d). Materials assigned to A or Oa horizons tended to exhibit strong medium to coarse subangular blocky or moderate to strong medium or coarse platy structure (Fig. 3a–d), remaining from lenticular cryostructures formed by ice lenses. Mineral horizons with low organic matter content tended to exhibit strong fine angular blocky cryogenic structure (Fig. 3a, 3d).

Soil pH in H_2O (pH_{H2O}) ranged from 3.6 to 7.9 and from 3.3 to 7.6 in $CaCl_2$ (pH_{CaCl2}) across all samples. Values for pH_{H2O} and pH_{CaCl2} were linearly related ($pH_{CaCl2} = 0.999 \times pH_{H2O} - 0.287$; $R^2 = 0.99$; $p < 0.0001$), with an average difference of 0.29 ± 0.14 pH units (pH_{H2O} - pH_{CaCl2}). The pH differed significantly between material types ($p < 0.0001$; one-way ANOVA F-test) (Table 1). Organic soil materials had significantly lower pH_{H2O} values than mineral soil materials (Table 1); however, fibric (Oi, $pH_{H2O} = 4.49 \pm 0.65$) and hemic (Oe, $pH_{H2O} = 4.91 \pm 0.60$) organic materials had significantly lower pH values than sapric organic materials (Oa, $pH_{H2O} = 5.79 \pm 0.41$) and all mineral material types (Table 1). This dramatic difference between the pH of the least decomposed organic materials near the soil surface (Oi and Oe horizons) and the sapric or mineral soil materials below led (on average) to an abrupt increase in pH with depth around 15 cm (Supplemental Fig. S2) followed by a nearly linear increase with increasing depth to pH values >7 (Supplemental Fig. S2).

Field textures and laboratory-determined particle size distributions revealed a thin, discontinuous, silty to very fine sandy mantle with an average thickness of 11 cm (range, 0–35 cm). This thin eolian layer was not recognized in all profiles and was difficult to identify in the field because it was typically located below the surficial organic materials in highly organic A horizons above the lacustrine sediments. Grain count data from the fine and very fine sand fractions of the eolian sediments from profiles where a thin loess cover was recognized show slightly higher glass percentages (Supplemental Table S2) than the lacustrine sediments below, but mineralogy in these fractions does not differ widely, suggesting that this material is eolian in nature and not volcanic ash. Soil textures in lacustrine materials ranged from 14 to 78% clay (average, 40 ± 14% clay) and were dominated by clays and silty clays (48% of samples) or clay loams and silty clay loams (43% of samples). The remaining 9% of soil textures in the lacustrine parent materials were loams, sandy loams, or sandy clay loams.

Soils across all 22 sites were classified as Gelisols (Supplemental Table S3). Of these 22 soils, four (18%) were classified as Histels, and 18 (82%) were classified as Turbels. The Histels were all dominated by sapric materials in the upper tier (Sapristels), and all had mineral contact within 1 m (Terric Sapristels). Of the Turbels, two (11%) were Aquiturbels (without a histic epipedon), and 16 (89%) were Histoturbels (with a histic epipedon). Depth-averaged sand and clay percentages in the particle size control section of Turbels (25–100 cm) and Histels (30 below the soil surface) demonstrate the variability in the underlying lacustrine sediments because six soils had <35% clay in the particle size control section (Supplemental Table S4). Family particle size classes were therefore unequally distributed because four of the Turbels (22%) classified as fine-loamy, whereas the remainder (78%) classified as fine. Among the Histels, two were loamy (66%), and one was clayey (33%) (Supplemental Table S3). All of the described soils

Table 1. Bulk density, soil organic carbon (SOC), and pH for generalized horizon groupings in soils under late-successional black spruce in the Copper River Basin, AK.

	n†	Bulk density	SOC	pH (1:1 H_2O)
		g cm^{-3}	g 100 g^{-1}	
Final horizon designation‡				
Oi	25, 26, 26	0.14 ± 0.04§A¶	38.0 ± 8.0A	4.49 ± 0.65A
Oe	13, 14, 14	0.21 ± 0.07AC	36.6 ± 5.7A	4.91 ± 0.60A
Oa	39, 42, 42	0.48 ± 0.17BD	21.8 ± 4.4B	5.79 ± 0.41B
A	4, 7, 7	0.57 ± 0.08CDE	12.0 ± 1.4CD	6.17 ± 0.32BCD
A/Cjj, C/Ajj (unfrozen at sampling)	29, 44, 44	1.22 ± 0.32F	3.9 ± 4.5EF	6.34 ± 0.45C
A/Cjj, C/Ajj (frozen at sampling)	52, 56, 56	0.89 ± 0.28E	3.1 ± 2.8E	6.80 ± 0.58D
C (unfrozen)	2, 3, 3	0.83 ± 0.13EF	3.0 ± 2.3DEF	6.39 ± 0.41BCD
C (frozen)	12, 14, 14	1.18 ± 0.31FG	0.8 ± 0.5F	7.16 ± 0.36D
Field-assigned horizon nomenclature#				
Organic (Oi, Oe, Oa)	58, 61, 61	0.28 ± 0.21A	33.3 ± 8.1A	5.04 ± 0.80A
Transitional (OaA, AOa)	19, 20, 20	0.46 ± 0.14A	18.1 ± 3.9B	5.94 ± 0.40B
Mineral (A)	5, 8, 8	0.56 ± 0.10A	13.0 ± 6.8C	5.98 ± 0.53BC
Mineral (C, A/Cjj or C/Ajj) unfrozen	30, 47, 47	1.22 ± 0.31B	2.8 ± 2.6D	6.38 ± 0.45C
Mineral (C, A/Cjj or C/Ajj) frozen	64, 70, 70	0.95 ± 0.31C	2.7 ± 2.7D	6.86 ± 0.56D

† The *n* column represents the number of samples analyzed for a property (bulk density, SOC, and pH, respectively). In some situations, there are fewer samples analyzed for bulk density than SOC because of the difficulty in obtaining reliable bulk density samples from some horizons. Although 220 physical samples were collected from the field, only 206 sample values are represented in this table because duplicate samples in some horizons were averaged to generate a horizon average value.

‡ Final horizon designations following review of field notes and laboratory analysis of samples for carbon and particle size distribution.

§ Averages reported represent arithmetic means ±1 SD.

¶ Within columns, rows with the same letters are not significantly different ($\alpha > 0.05$, Tukey's HSD).

Field-assigned horizon nomenclature prior to laboratory analysis of samples.

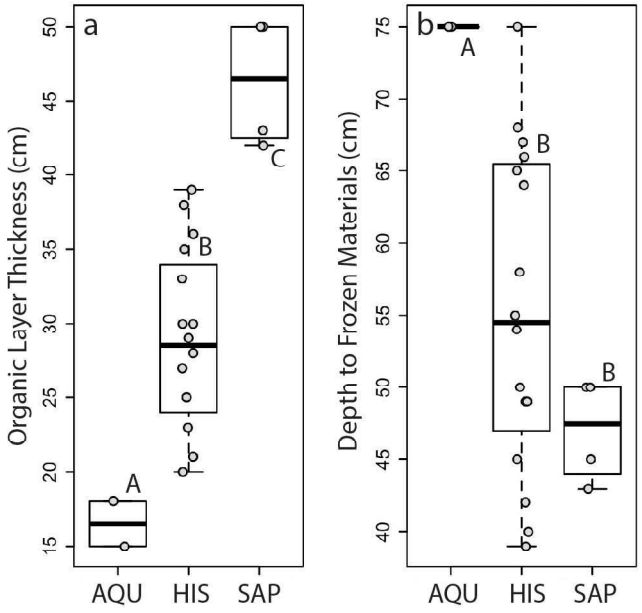

Fig. 4. Boxplots of (a) organic layer thickness and (b) depth to frozen materials at the time of sampling under late-successional black spruce in the Copper River Basin, AK, by Great Group (Soil Survey Staff, 2014b). Categories with the same capital letters are not significantly different (α > 0.05, Tukey's HSD). AQU, Aquiturbels; HIS, Histoturbels; SAP, Sapristels.

were non-acid or euic according to pH guidelines in *Keys to Soil Taxonomy* (Soil Survey Staff, 2014b) (Supplemental Table S3).

The OLT was significantly greater in Histels (+18 cm) than in Turbels (p < 0.001; Tukey's HSD) and differed significantly between all three observed great groups (p < 0.001; Tukey's HSD) (Fig. 4). Sapristels had an average OLT of 46 ± 4 cm, Histoturbels had an average OLT of 29 ± 6 cm, and Aquiturbels had an average OLT of 17 ± 2 cm (Fig. 4). Depth to frozen materials was not significantly different between Suborders (p > 0.1; Tukey's HSD); however, among Great Groups, Aquiturbels had significantly deeper depths to frozen materials than Histoturbels (+19 cm) and Sapristels (+28 cm) (p < 0.04 and 0.01, respectively; Tukey's HSD) (Fig. 4). Depth to the estimated bottom of the transient layer did not differ significantly between Suborders or Great Groups (p > 0.01; Tukey's HSD).

Cryostructures in Near-Surface Permafrost

Across all 22 investigated soils, a total of 84 morphological horizons were described in frozen materials. Of the 84 horizons described in frozen materials, 17 (20%) were weakly frozen, with no recognizable cryostructure but distinct, weakly aggregated ice crystals at the time of sampling. Among the remaining 67 frozen morphological horizons, four major types of cryostructures were described: suspended (ataxitic) (n = 10; 12% of total) (Fig. 5a–d), lenticular (n = 37; 44% of total) (Fig. 5e–h), micro-lenticular (n = 16; 19% of total) (Fig. 5i–l), and massive (pore ice) (n = 4; 5% of total) (Fig. 5m–p).

Cryostructure types differed significantly in the depth at which they were observed (one-way ANOVA F-test; p = 0.018) (Fig. 6). Lenticular and micro-lenticular cryostructures were observed across depths from 43 to 126 cm (average, 85 ± 21 cm and 93 ± 22 cm, respectively), suspended cryostructures were observed predominantly near the top of the permafrost table (average, 71 ± 19 cm) (Fig. 7), and massive cryostructures were typically observed in much deeper increments (average, 105 ± 8 cm) (Fig. 7). Massive and micro-lenticular cryostructures were present at significantly lower depth increments than macro-lenticular and suspended cryostructures (p = 0.03 and 0.05, respectively; Tukey's HSD) (Fig. 6 and 7). Among frozen horizons with defined cryostructures (excluding weakly frozen horizons) that were sampled and analyzed in the laboratory (n = 57), volumetric water content varied significantly by cryostructure type (p < 0.001; one-way ANOVA F-test) (Fig. 6). Suspended cryostructures contained, on average, 12% more water by volume than lenticular cryostructures (p = 0.03; Tukey's HSD), whereas suspended types contained, on average, 26 and 18% more volumetric water than massive and micro-lenticular types (Fig. 6).

Relationships between Soil Properties and Variation by Horizon Type

Empirical functions developed for future local modeling and gap-filling in the late-successional black spruce soils investigated in this study are shown in Fig. 8. Total N was nonlinearly related to SOC across the subset of samples (n = 138) analyzed for C and N by dry combustion (Fig. 8a) and best modeled using a nonlinear Michaelis–Menten function (Archontoulis and Miguez, 2015). Soil organic C by dry combustion was linearly related to LOI (R^2 = 0.994; p < 0.001) (Fig. 7b). The SIC content increased rapidly above pH values of 6.5 (Fig. 8c), but all samples had relatively low SIC contents (<0.8%).

For unfrozen materials (both organic and mineral), LOI was the single most important variable for predicting bulk density (Fig. 9a). In attempts with multiple regression, no other variables were significant after LOI was included the model. The best-fit model was a logarithmic function (Fig. 9a). For frozen samples, gravimetric ice content was the best predictor of bulk density also with a nonlinear logarithmic function (Fig. 9b).

Bulk density and SOC differed between generalized categories of horizons (p < 0.0001 in both cases, one-way ANOVA F-test) (Table 1). Fibric (Oi) and hemic (Oe) materials were not significantly different from each other in either bulk density or SOC but were significantly lower in bulk density (0.14 and 0.21 g cm^{-3}) and higher in SOC (38 and 36%) than sapric materials (Oa) (0.48 g cm^{-3} and 21.8% SOC) (Table 1). Cryoturbated horizons (A/Cjj, C/Ajj) were significantly higher in bulk density than organics and A horizons (with the exception of frozen cryoturbated horizons, which were not significantly different from A horizons) and lower in SOC (Table 1).

Water Content, Bulk Density, and Soil Organic Carbon Depth Profiles

Aggregated depth profiles of water content (gravimetric [θ_g] and volumetric [θ_v]), bulk density, and SOC demonstrated related trends with depth. Average θ_g at the time of sampling was highest in surficial organic materials (Fig. 10a) and abruptly declined to a minimum of 50% at 55 cm (corresponding to the

Fig. 5. Typical cryostructures observed in near-surface permafrost under late-successional black spruce in the Copper River Basin, AK. (a–d) Suspended (ataxitic); (e–h) lenticular; (i–l) microlenticular; (m–p) massive (pore ice).

average depth to observed frozen materials across all 22 sites) before increasing again to an average of 91% at 88 cm in the zone interpreted as the upper permafrost (Fig. 10a). Average θ_v peaked in the lower organic layers (due to the extremely low bulk density of the upper organic layers at 18 cm) before declining to a minimum of 51% at 55 cm and increasing again to a maximum of 68% at 88 cm (Fig. 10b). Average bulk density was lowest in the surficial organic materials and increased rapidly through the upper mineral soil materials to a maximum of 1.2 g cm^{-3} at 55 cm before declining rapidly to a minimum of 0.85 g cm^{-3} at 88 cm and subsequently increasing with depth (Fig. 10c). The SOC concentrations were highest in the surficial organic horizons and exhibited a generally decreasing trend with depth. However, that trend slowed between 55 and 100 cm due to the presence of cryoturbated A horizon materials, corresponding to the upper permafrost (Fig. 10d).

Cryoturbation

Cryoturbation was a common feature of all investigated soils. Of 206 described morphological horizons, 129 were mineral, and of those mineral horizons only 17 (13%) did not show morphological indications of cryoturbation or the presence of gelic materials (Soil Survey Staff, 2014b). Evidence of extensive cryoturbation in these soils ranged from features appearing to indicate solutioning processes through the downward movement of saturated organic-rich materials or porewaters (Fig. 11a–c), streaking of organic rich materials moving vertically downward into macropores (Fig. 11d, 11e), and the mass movement of organic-rich mineral materials (i.e., A horizon materials) into the subsoil (Fig. 11f–k). In the near-surface permafrost, cryostructures were overprinted on these cryoturbated features (Fig. 11i–k), suggesting that cryoturbation occurred prior to modern cryostructure formation.

The volume percentage of A horizon material in cryoturbated horizons estimated in the field was nonlinearly related to the SOC percentage in the bulk horizon (Fig. 12a). The combined probability of A horizon volume percentage with depth across all sites decreased from a maximum of 0.68 at 38 cm to <0.1 below 125 cm (Fig. 12b). Across all sites, 19 samples were taken of individual A or C components within horizons. The SOC concentrations of the A component of these samples (n = 10) ranged from 1.3 to 14.8% (average, 6.7 ± 4.9%), whereas SOC concentrations of the C component of these samples (n = 9) ranged from 0.8 to 2.8% (average, 1.4 ± 0.7%). The SOC concentrations of bulk grab samples corresponding to a subset of horizons (n = 8) averaged 1.9 ± 1.6%. For horizons where subsamples of both individual A and C components were taken, the SOC ratio of the A component to the C component ranged from a maximum of 11.9 to a minimum of 0.3, and there was a decreasing trend in this ratio with depth (Fig. 12c). None of the C-rich components of the horizons met the criteria for inclusion in organic soil materials (i.e., sapric, Oa materials), and all were thus assigned an A master designation.

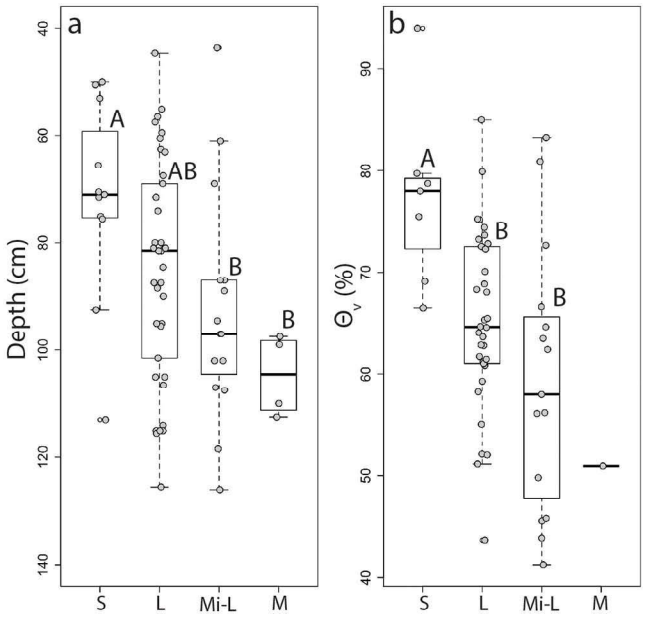

Fig. 6. Boxplots of cryostructure types under late-successional black spruce in the Copper River Basin, AK, with (a) average depth of observation and (b) volumetric ice content for those horizons where physical samples were analyzed in the laboratory. Categories with the same uppercase letters are not significantly different ($\alpha > 0.05$, Tukey's HSD). L, lenticular; M, massive (pore ice); Mi-L, microlenticular; S, suspended (ataxitic).

Carbon Stocks

The SOC stocks to 1 m averaged 46 ± 12 kg m^{-2} across all 22 sites (Supplemental Table S3). On average, 56 ± 14% of the total 1-m stock was contained in organic materials, whereas 44 ± 14% of the total 1-m SOC stock was contained in cryoturbated mineral materials (range, 9–67%) (Supplemental Table S3). The OLT was a critical predictor of 1-m SOC stocks (R^2 = 0.325; p < 0.001) (Fig. 13). No other site factors were significant predictors of 1-m SOC stocks once OLT was present in the model.

The SOC stocks were significantly greater in Histels than in Turbels (+15 kg SOC m^{-2}) (Tukey's HSD; p = 0.016) and significantly greater in Sapristels than Aquiturbels (+30 kg SOC m^{-2}) (Tukey's HSD; p = 0.004) but did not differ between Histoturbels and Aquiturbels or Sapristels (Fig. 14). The percentage of the 1-m SOC stock contained in organic materials was significantly greater in Histels than in Turbels (+25%) (Tukey's HSD; p < 0.001). Histels contained, on average, 22 kg m^{-2} more SOC in organic materials to 1 m depth than Turbels (p < 0.0001; Tukey's HSD), but there was no significant difference between Histels and Turbels regarding the stock of C in cryoturbated mineral materials to 1 m. When normalized by OLT thickness, Histels contained on average 0.16 kg m^{-2} more SOC in organic materials per centimeter of organics than Turbels (p = 0.04; Tukey's HSD). Sapristels contained a significantly higher proportion of 1-m SOC stocks in organic materials than Aquiturbels and Histoturbels (Fig. 14). When normalized by the thickness of cryoturbated mineral materials, the amount of SOC contained per centimeter of cryoturbated mineral materials (0.12 kg m^{-2} for Histels and Turbels) was not significantly different between suborders.

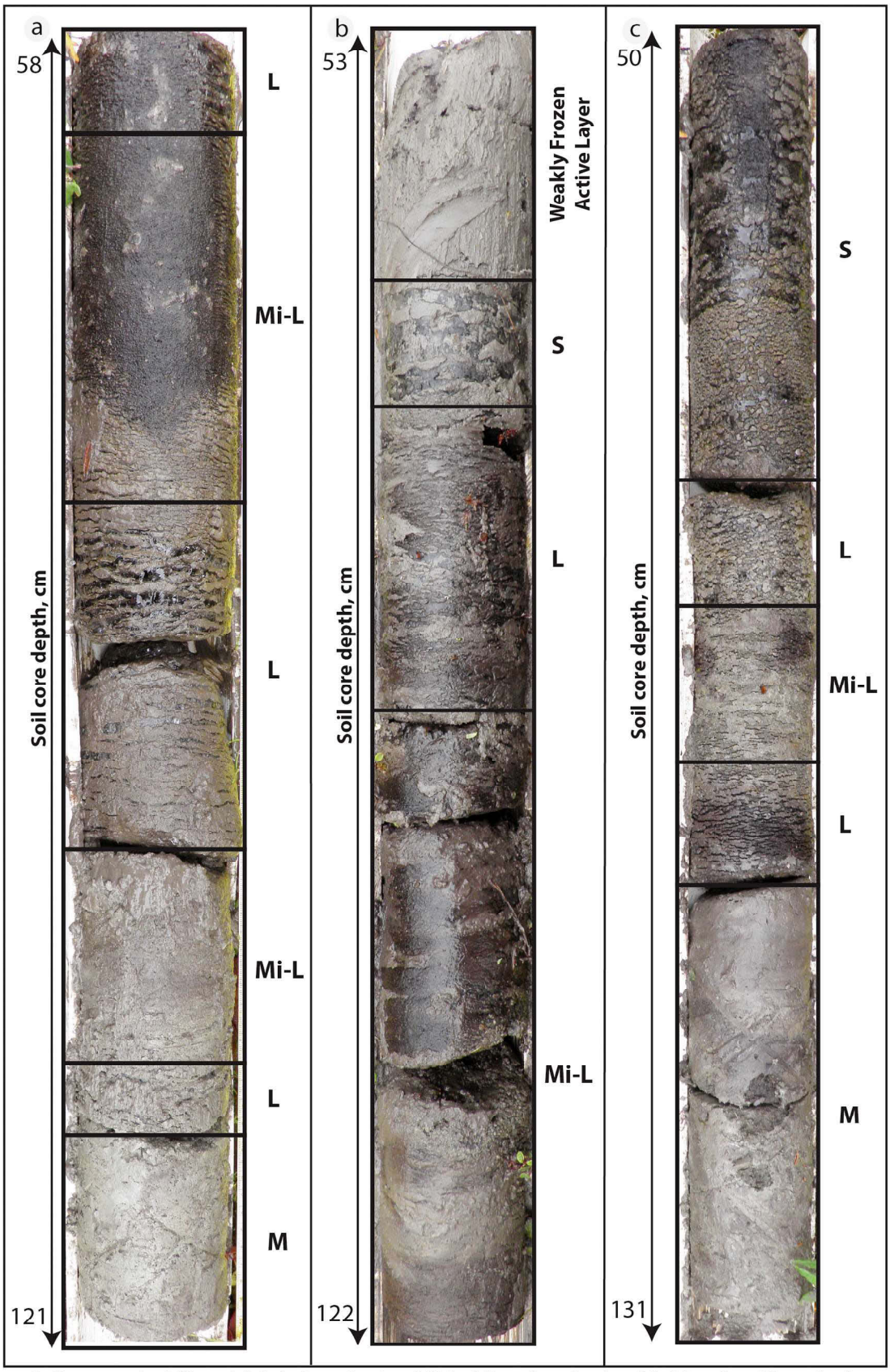

Fig. 7. Typical patterns of cryostructures in near-surface permafrost under late-successional black spruce in the Copper River Basin, AK, demonstrating general patterns of decreasing ice content with depth. Each of these cores was taken with a US Snow, Ice and Permafrost Research Establishment corer and was frozen at the time of sampling at the top of the core. (a, b) Microlenticular cryostructures typical of organic-rich cryoturbated materials and lenticular cryostructures typical of mineral soil materials. (b, c) Suspended cryostructures present in the transient layer of the upper permafrost. (a, c) Massive cryostructures in the lower portion of each core.

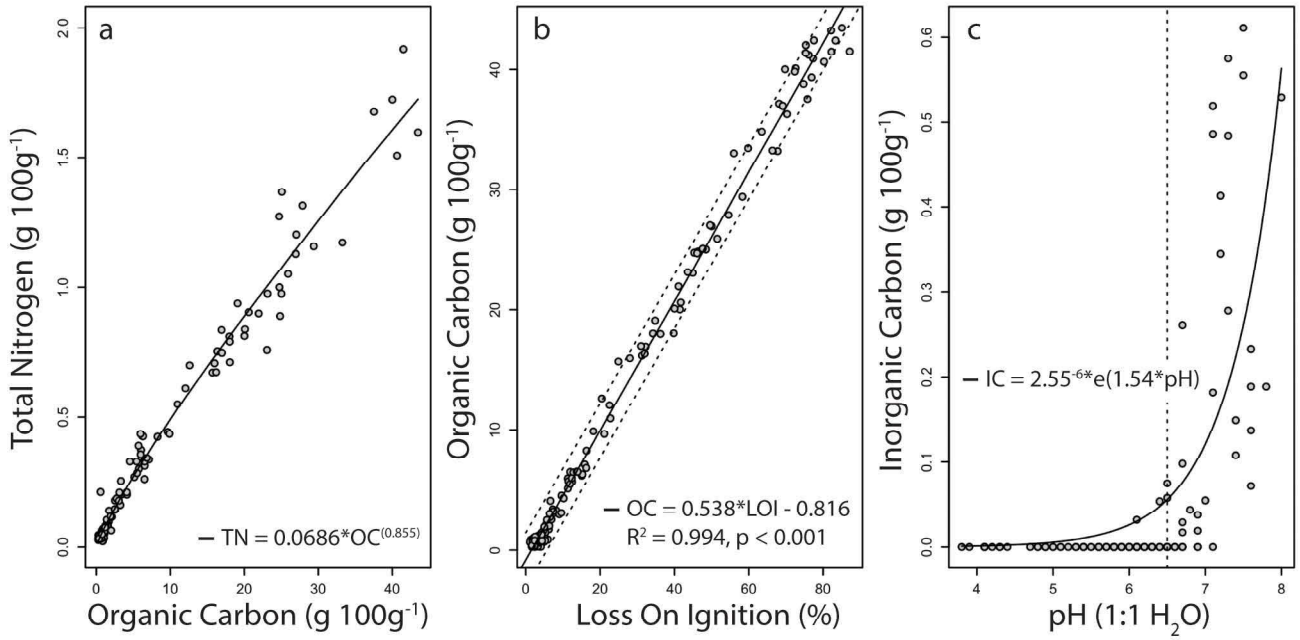

Fig. 8. Derived relationships between soil properties for soils under late-successional black spruce in the Copper River Basin, AK. (a) Soil organic carbon and total nitrogen using a nonlinear Michaelis–Menten model (Archontoulis and Miguez, 2015). (b) Loss on ignition and soil organic carbon using a linear model. Dotted lines represent the 99% prediction interval around the slope of the linear regression line. (c) pH and soil inorganic carbon using a power model (Archontoulis and Miguez, 2015).

DISCUSSION

Morphological Criteria and Field Determination of Horizon Nomenclature and Classification

The thickness of organic materials (i.e., OLT) in permafrost-affected soils under black spruce is a critical site metric (Fisher et al., 2016; Gewehr et al., 2014) because it is related to soil classification (Soil Survey Staff, 2014b), active layer depth (O'Donnell et al., 2011), and predictive models of 1-m SOC stocks (Fig. 13) (Michaelson et al., 2013; O'Donnell et al., 2011). In many studies, OLT is typically assessed in the field, and a subjective decision must be made to determine whether or not a given material is mineral or organic, despite the need for both SOC and texture data to make this determination categorically, according to established criteria (Soil Survey Staff, 2014b). This is especially true of the soils in this study, which were characterized by organic materials that graded subtly into mineral materials with depth.

Of the horizons that were assigned an A master in the field in this study, only 6 of 15 (40%) met the criteria for mineral soils after laboratory analysis. Once SOC and particle size distribution data were obtained, only 2 of 20 (10%) met the criteria for mineral soil materials. Therefore, of the total number of soil horizons assigned either A nomenclature or OA/AO transitional nomenclature in the field, only 8 of 35 (23%) met the criteria for mineral soil materials after laboratory analysis. This means that it is likely that these transitional horizons feel denser (perhaps because of their greater water weight in the field), and thus (at least in the poorly to very poorly drained soils in the CRB) it may be best to err on the side of organic materials in the field if forced to make a binary choice for classification purposes when evaluating materials.

Relationship of Organic Layer Thickness to Previous Studies of Soils under Black Spruce and Relationship to Site Factors

O'Donnell et al. (2011) reported a nonlinear exponential relationship between OLT and observed depth to frozen materials across a post-fire chronosequence on soils under black spruce in the interior. In a study in the Canadian Great Slave lowland region, 24 sites under late-successional black spruce on fine-textured soils with moderate slopes (average, 6.8%) had three key driving factors that determined late season depth to frozen materials at the time of sampling: soil surface moisture, tree canopy leaf area index, and OLT (Fisher et al., 2016). Although a significant linear relationship between depth to frozen materials and OLT existed across all sites in this study of late-successional soils in the CRB (Fig. 2), live tree density and soil moisture were not significantly related to thaw depth ($p > 0.2$ in both cases).

On average, OLT at (31 ± 10 cm) was greater than that reported in previous studies under late-successional black spruce on somewhat poorly drained and poorly drained soils formed in loess in the Alaskan interior (22 cm [Ping et al., 2010]; 24 cm [O'Donnell et al., 2011]). However, the OLTs observed were consistent with very poorly drained soils under black spruce reported across the interior (35.5 ± 32 cm; Ping et al., 2010). Although OLT reported in this study was comparable with very poorly drained soils in the interior, the depth to frozen materials (56 ± 12 cm) and depth to the bottom of the transient layer (69 ± 19 cm) reported in this study are deeper than those reported in other studies from the interior (44 cm [Ping et al., 2010]; 45 cm [O'Donnell et al., 2011]). These observations do, however, align broadly with the observed depth to permafrost (54 cm) for one previously investigated site under late-successional black spruce in the CRB (Clark and Kautz, 1999).

The deeper depths to frozen materials reported here, despite increased OLT in comparison to other studies, could be due to several interacting factors. First, these differences may be due to interannual variability of active layer depth because the observations reported in this study and previous studies in the CRB span large temporal ranges (i.e., Clark and Kautz, 1999; Ping et al., 2010). Second, because the lower portion of the organic materials observed in this study are typically dense, high-water-content transitional materials, it is likely that they have higher thermal conductivity and may thus facilitate deeper thermal transfer during the growing season. Hydrology and decomposition state could therefore be major driving factors because the thermal conductivity of organic materials increases significantly with increased water content and decomposition state (O'Donnell et al., 2009). Finally, there is a possibility that the deeper depths to frozen materials observed in this work are a result of long-term changes in climate because the observations reported here were taken one to three decades after the observations reported in O'Donnell et al. (2011) and Ping et al. (2010) and because Alaska continues to experience warming trends that can lead to increases in active layer depths (Jafarov et al., 2012).

Relationships between Soil Properties

The bulk densities and SOC concentrations of major horizon groupings reported here are broadly consistent with those reported in previous studies on soils under black spruce formed on loess in the Alaskan interior (O'Donnell et al., 2011), although the measured bulk densities of organic materials in this study tended to be higher. The bulk densities of fibric and sapric organic materials across the sites in this study (averages, 0.14 and 0.48 g cm^{-3}, respectively) are higher than the bulk densities reported in O'Donnell et al. (2011) for analogous materials (0.05 and 0.23 g cm^{-3}, respectively) despite similar SOC concentrations. However, the bulk densities of active layer and upper permafrost mineral materials (averages, 1.22 and 0.89 g cm^{-3}) were similar to those reported in O'Donnell et al. (2011) (1.23 and 0.70–0.92 g cm^{-3}, respectively). Average SOC concentrations of active layer mineral

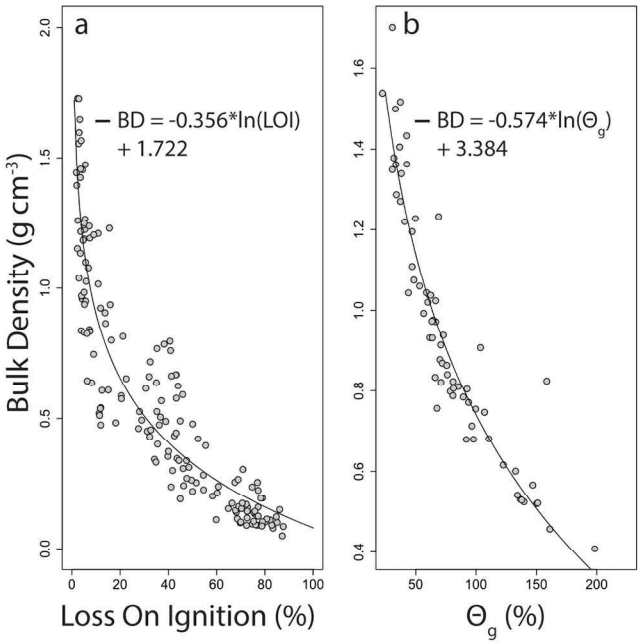

Fig. 9. Derived nonlinear relationships using a logarithmic function (Archontoulis and Miguez, 2015) between bulk density (BD) and (a) loss on ignition (LOI) for unfrozen mineral and organic samples and (b) BD and gravimetric ice content for frozen samples for soils under late-successional black spruce in the Copper River Basin, AK.

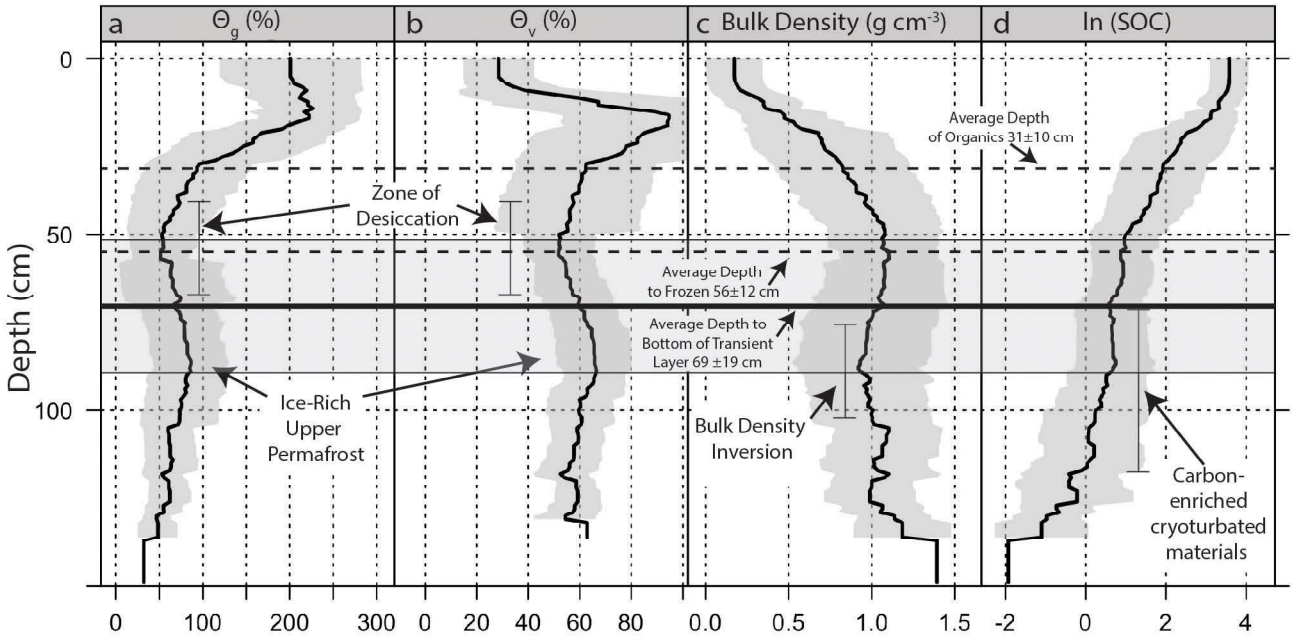

Fig. 10. Depth profiles of average (a) gravimetric water content, (b) volumetric water content, (c) bulk density, and (d) soil organic carbon (SOC; natural log used for visualization and scaling purposes) in soils under late-successional black spruce in the Copper River Basin, AK. Black line represents "slabbed" averages for every 1-cm increment across all sites (using the AQP package in R [Beaudette et al., 2013]). The gray zone represents 1 SD from the mean.

Fig. 11. Morphological evidence of cryoturbation observed in Copper River Basin soils under late-successional black spruce. (a–c) Solutioning and downward movement of saturated organic (Oa, sapric) and mineral (A) horizon materials in the active layer. (d–f) Streaking and downward movement of organics through macropores. (g) Cryoturbated materials in the active layer. (h–k) Frozen cryoturbated materials with "overprinting" of lenticular or microlenticular cryostructures on previously cryoturbated materials.

materials reported in this study (3.9%) were also very similar to those reported in O'Donnell et al. (2011) (3.4%).

The best predictor for the bulk density of frozen materials was gravimetric water content (Fig. 9b), and once water content was in the equation, SOC was not significant (multiple linear regression; $p > 0.3$). For unfrozen soil materials (including organic materials and unfrozen mineral soil materials in the active layer) in this study, LOI was the best predictor of bulk density (Fig. 9a), and no other variables were significant once LOI was in the model. After converting LOI values to predicted SOC for all samples in this study, the resulting bulk density model [−0.296 ln(%SOC) + 1.30] is similar to that reported in a meta-analyses for all Alaska Gelisols [−0.295 ln(%SOC) + 1.36] (Michaelson et al., 2013) but differs significantly for Gelisol active layer materials only [−0.334 ln (%SOC) + 1.57] (Michaelson et al., 2013). It thus appears that using the database equation for all Alaskan Gelisols (Michaelson et al., 2013) would overestimate bulk densities of active layer materials for soils under late-successional black spruce in the CRB. This underscores the importance of using local data and regressions for gap filling whenever possible.

Near-Surface Permafrost Morphology

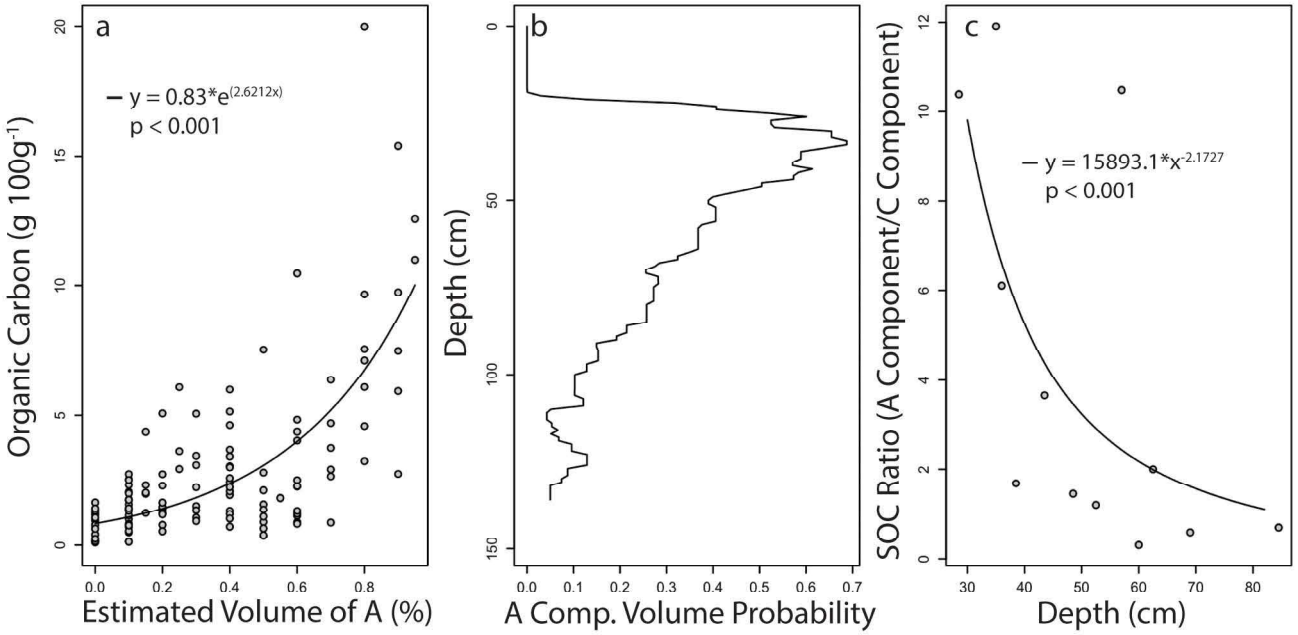

Fig. 12. Patterns in cryoturbation in soils under late-successional black spruce in the Copper River Basin, AK. (a) relationship between field morphological estimates of A component prevalence in cryoturbated horizons and the soil organic carbon (SOC) for bulk samples of cryoturbated horizons using a nonlinear power model (Archontoulis and Miguez, 2015). (b) Average A horizon component probability by 1-cm depth increments across all soils illustrating slowly decreasing prevalence of cryoturbated A horizon materials with depth. (c) The SOC ratio of A components and C components of cryoturbated horizons (*n* = 12) with depth modeled using a nonlinear logarithmic function (Archontoulis and Miguez, 2015).

and Characteristics

Consistent with previous studies showing the predominance of lenticular cryostructures in glaciolacustrine deposits (Shur and Zhestkova, 2003), the majority of the observed near-surface cryostructures in this study (82% of non-weakly frozen horizons) were lenticular. In contrast to O'Donnell (2010), who studied cryostructures in near-surface permafrost in para-syngenetically formed lacustrine sediments in the Koyukuk Flats (Alaskan interior), inclined ice lenses were not observed in this study. Unlike colder, drier environments where vertical cracking and reticulate cryostructures are more common in near-surface permafrost (Ping et al., 2008, 2015), vertical cracks in the near surface permafrost were not observed in this study.

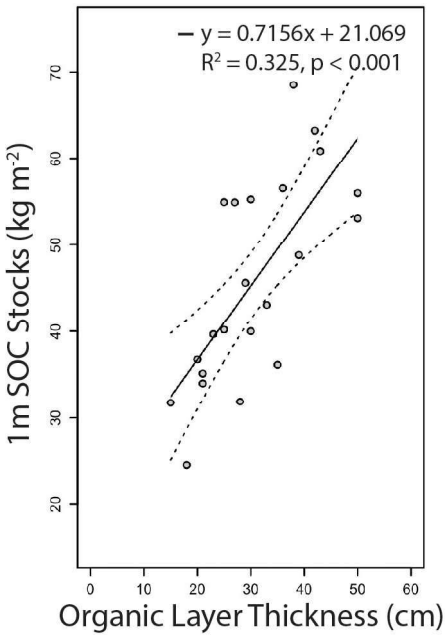

Fig. 13. Relationship between organic layer thickness and 1-m soil organic carbon (SOC) stocks across all investigated soils (*n* = 22) under late-successional black spruce in the Copper River Basin, AK. The dotted lines represent the 95% confidence interval around the slope of the linear regression line.

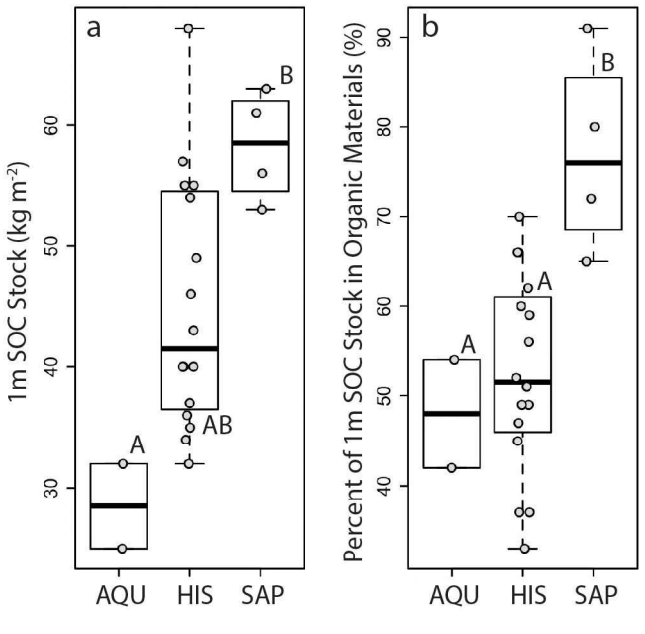

Fig. 14. Boxplots of (a) soil organic carbon (SOC) stocks to 1 m depth and (b) percentage of 1 m SOC stocks contained in organic materials under late-successional black spruce in the Copper River Basin, AK by Great Group (Soil Survey Staff, 2014b). Categories with the same uppercase letters are not significantly different ($\alpha > 0.05$, Tukey's HSD). AQU, Aquiturbels; HIS, Histoturbels; SAP, Sapristels.

Whereas the depth to frozen materials reported in this study was related to the OLT at each site (Fig. 2), the estimated depth to the bottom of the transient layer was not significantly correlated with OLT or any other site factors (linear regression; $p > 0.3$). Depth to frozen materials (one-way ANOVA F-test; $p < 0.01$) differed significantly between Great Groups (Fig. 4) but not depth to the bottom of the transient layer (one-way ANOVA F-test; $p > 0.2$). The observed lack of correlation between the depth to the bottom of the transient layer and OLT in this study could indicate that the transient layer is recording longer-term processes (French and Shur, 2010) and is broadly comparable across similar sites under late-successional black spruce in the CRB regardless of current OLT.

Mechanisms of Cryoturbation: Relationship to Depth Patterns of Soil Properties

The soils investigated in this study show trends consistent with the general observation that, on average, water content decreases above the permafrost table in a zone of desiccation before increasing in the upper permafrost (French and Shur, 2010; Ping et al., 2015; Shur and Jorgenson, 2007). This has a key influence on patterns in bulk density with depth, which show an increase in the lower active layer before decreasing in the upper permafrost due to increasing ice content. Similar to other studies, the bulk density of soil materials in the upper permafrost in this study was lower than that of mineral soil in the active layer (Fig. 10; Table 1) (O'Donnell et al., 2011). A slowing trend in SOC decrease was observed in the upper permafrost (Fig. 10), consistent with the accumulation of organic-rich materials in the upper permafrost due to cryoturbation (Ping et al., 2015) but less dramatic than the strong, increasing trend in SOC concentrations at the permafrost table that has been observed in other cryoturbated soils in the Arctic (Kaverin, 2008; Ping et al., 2010).

Studies on the morphological outcomes of cryoturbation have overwhelmingly focused on the Arctic, where patterned ground predominates and frost-cracking is a dominant mechanism of cryoturbation (Ping et al., 2015; Reiger, 1983; Shur et al., 2008). Although soils under late-successional black spruce in the CRB are fine textured and have thick insulating organic layers and poor drainage, all of which should inhibit the frost-cracking mechanism of cryoturbation (Carter and Bentley, 1991; Palmtag and Kuhry, 2018; Reiger, 1983), they are characterized by the presence of cryoturbated materials to depths of up to 150 cm, often well below the current permafrost table (Fig. 7, 10–12; Supplemental Table S3). In the absence of frost-cracking, cryoturbation mechanisms in these soils would therefore require periodic deepening of the active layer. It is highly unlikely that interannual variability in thaw depths in these soils could account for variability this extensive, based on borehole data from a nearby site under black spruce (Gakona 1), where, during the 8-yr period from 2010 to 2017, active layer thickness remained between 58 and 66 cm (GIPL, 2019).

It is therefore likely that much of the active cryoturbation in these soils is due to solutioning or organic matter "retinization" (the downward movement of saturated organic materials, sensu) (Dimo, 1965) and/or diapirism (the upward movement of less dense materials through a denser overlying layer; e.g., Swanson et al. [1999]) after post-fire active layer deepening. Typically, permafrost degradation after fire disturbance occurs not from the immediate effects of heat conduction into the ground but rather from the loss of a portion of the insulating organic layer and subsequent albedo change (Jiang et al., 2015; Yoshikawa et al., 2003). The effects of fire on active layer thickness in black spruce systems varies depending on fire severity, but active layer thicknesses can increase by a factor of 3 to 5 if the loss of the surface organic layer is extensive (Dyrness, 1982). Regions such as the CRB that have relatively warm near-surface permafrost (within 1°C of 0°C) can be particularly vulnerable to thaw and degradation after disturbance (Nelson et al., 2001). In a study on burned and unburned sites under black spruce 2 yr after 2015 fires in the Alaskan interior near Tanana Flats, a difference in temperature of up to 10°C after fire was observed at a depth of 30 cm, and depth to frozen materials on burned sites was >40 cm deeper than those of adjacent unburned sites (Potter and Hugny, 2018). Depth to permafrost under black spruce was observed to increase by 40 and 60 cm 1 and 2 yr, respectively, after the Wilson Camp Fire in 1981 east of Glennallen and Copper Center, in the CRB (Clark and Kautz, 1999). Active layer thicknesses can continue to increase for at least an additional decade after fire disturbance, until the insulating organic layer begins to recover (Viereck and Dyrness, 1979).

Under a stable climate, aggradation of the permafrost table can occur naturally because the recovery of the surficial organic layer provides increasing insulation (i.e., Shur and Jorgenson, 2007). The prevalence of lenticular cryostructures "overprinted" on cryoturbated materials observed in this study (Fig. 7) suggests that cryoturbation occurred during periods of thaw followed by aggradation of the permafrost table. This means that the organic-rich materials that are being cryoturbated into the mineral soil tend to be well decomposed and from the lower portion of the organic layer, which is more likely to be transitional between mineral and organic materials. These proposed mechanisms are also supported by the depth distribution of bulk density (Fig. 10c) and by a rapidly decreasing ratio of SOC in A component materials relative to adjacent C component materials with depth (Fig. 12c). In soils under black spruce in the CRB, it is therefore likely that cryoturbation may occur in cycles associated with fire, when both dynamic active layer deepening and aggradation processes result in conditions that favor deeper mixing of C-rich materials.

Soil Organic Carbon Stocks and Carbon Partitioning

Stocks of SOC to 1 m depth under late-successional black spruce in this study averaged 45.5 ± 11.8 kg SOC m^{-2}, with 13.4 ± 12% of the SOC contained in materials that were frozen at the time of sampling. The 1-m SOC stocks reported for the 22 sites in this study (46 ± 12 kg SOC m^{-2}) (Supplemental Table S3) are in the general range of poorly drained and very poorly drained sites under black spruce throughout the Alaskan interior (Ping et al., 2010), which averaged 46 kg SOC m^{-2} ($n = 19$) and 51 kg SOC m^{-2} ($n = 6$), respectively. These 1-m SOC stocks are relatively high in the

context of SOC stocks across the state of Alaska for non-Histosols or Histels (Johnson et al., 2011) and are much higher than 1-m SOC stocks reported in larch-dominated forests in Siberia (11 kg SOC m^{-2}) (Webb et al., 2017), soils under black spruce formed in loess in interior Alaska (average, 17.1 kg SOC m^{-2}) (O'Donnell et al., 2011), and previously reported for a site under black spruce in the southern CRB (20.7 kg SOC m^{-2}) (Ping et al., 2010).

Organic layer thickness under late-successional black spruce in the CRB is a major driver of 1-m SOC stocks ($p < 0.001$) (Fig. 13), a result that is supported by previous work in black spruce soils in interior Alaska (O'Donnell et al., 2011). The percentage of 1-m SOC contained in organic materials in this study (56 ± 14%) differed significantly by Great Group (77% for Histels and 52% for Turbels) and was in line with poorly and very poorly drained sites reported in a statewide meta-analysis (57%) (Ping et al., 2010). An average of 44 ± 14% of the SOC stock to 1 m depth was contained in frozen and unfrozen cryoturbated horizons (range, 9–67%). Therefore, although OLT is an important predictor of 1-m SOC stock in the soils investigated, cryoturbation is also a critical process for generating total 1-m SOC stocks. With projected increases in fire frequency in Alaska (Kasischke and Turetsky, 2006; Kasischke et al., 2010) and high-latitude climate change (Collins et al., 2013), competing directions of impact could occur on permafrost-affected soils of the Copper River Basin. On one hand, increased fire frequencies could provide additional opportunities for cryoturbation to occur. However, given that OLT is a significant driver of SOC stocks in these soils (Fig. 13) and that surface organics serve to insulate and maintain near-surface permafrost, therby reducing decomposition, it is likely that these changes would reduce the overall SOC stocks in these soils through increased decomposition rates, loss of near-surface permafrost, and thinning of surface organic layers (Genet et al., 2013; O'Donnell et al., 2011).

CONCLUSIONS

Soils under late-successional black spruce in the CRB are well insulated and have developed on fine-textured lacustrine sediments with high clay contents and lower frost susceptibility than the silt-dominated soils of the Alaskan interior. However, cryoturbation remains an important and ubiquitous component of permafrost-affected soils in the CRB and, in addition to the formation of the surface organic layer, is a critical process for generating total SOC stocks. Evidence suggests that the main mechanisms of cryoturbation in these soils are solutioning and diapirism during periods of post-fire degradation and aggradation of the permafrost table. This is supported by (i) extensive observations of cryoturbated mineral materials found below the permafrost table with little to no evidence of vertical cracking and (ii) overprinting of lenticular cryostructures on cryoturbated mineral materials, suggesting permafrost aggradation after mixing. The results of this process across the landscape have resulted in the long-term generation of significant SOC stocks below the organic layer. Although OLT appears to be the major driver of SOC stocks, SOC is nearly evenly partitioned between organic materials and cryoturbated mineral horizons in the top 1 m. This demonstrates that these soils are highly dynamic and have the potential to be sensitive to changes in fire return intervals, burn intensity, vegetation change, and long-term changes in climate. Future work on permafrost-affected soils in the CRB should focus on quantifying the effects of fire on SOC stocks and SOC partitioning.

SUPPLEMENTAL MATERIAL

The Supplemental Material provided along with this manuscript provides additional details on background information related to the ecological context of the soils investigated in this study, such as associated ecological sites (Figure S1, Table S1), grain count methods, and data from soils typical of the study area (Text S1, Table S2). Information regarding soil classification and site characteristics (Table S3); coordinates of the sampling sites ($n = 22$); and particle size data and depth profiles of pH, sand, and clay from the study sites is also provided (Fig. S2; Table S4).

ACKNOWLEDGMENTS

This work was supported in part by UMN–MAES funding to N.A. Jelinski, USDA–NRCS Agreement #68-7482-15-531 to N.A. Jelinski, and a USDA–NRCS CIG grant to Ahtna, Inc. This work was completed by A. Williams outside of her official duty as an NRCS employee. The findings and conclusions in this publication are those of the author(s) and should not be construed to represent any official USDA or US Government determination or policy. The authors thank M.H. Clark, C.-L. Ping, and N. Parry for discussions about Copper River Basin soils; S. Daszkiewicz for assistance in the field; and S. Bauer and K. Ring for assistance in the laboratory. The authors thank two anonymous reviewers for their comments and suggestions which significantly imporved this article.

REFERENCES

Archontoulis, S.V., and F.E. Miguez. 2015. Nonlinear regression models and applications in agricultural research. Agron. J. 107:786–798. doi:10.2134/agronj2012.0506

Akaike, H. 1998. Information theory and an extension of the maximum likelihood principle. In: E. Parzen, K. Tanabe, and G. Kitagawa, editors, Selected papers of Hirotugu Akaike. Springer Series in Statistics (Perspectives in Statistics). Springer, New York. p. 199–213. doi:10.1007/978-1-4612-1694-0_15

Alaska Interagency Coordination Center. 2018. Alaska large fires database. https://fire.ak.blm.gov/predsvcs/maps.php (accessed 1 Sept. 2019).

Alaska Land Use Council. 1984. Susitna joint venture document 2447-III: Fire management information. Alaska Power Authority, Anchorage. www.arlis.org/docs/vol2/hydropower/APA_DOC_no._2446.pdf (accessed 1 Sept. 2019).

Beaudette, D.E., P. Roudier, and A.T. O'Geen. 2013. Algorithms for quantitative pedology: A toolkit for soil scientists. Comput. Geosci. 52:258–268. doi:10.1016/j.cageo.2012.10.020

Bennett, M.R., D. Huddart, and G.S.P. Thomas. 2012. Facies architecture within a regional glaciolacustrine basin: Copper River, Alaska. Quat. Sci. Rev. 21:2237–2279. doi:10.1016/S0277-3791(02)00027-6

Bockheim, J.G. 2007. Importance of cryoturbation in redistributing organic carbon in permafrost-affected soils. Soil Sci. Soc. Am. J. 71:1335–1342. doi:10.2136/sssaj2006.0414N

Carter, M., and S.P. Bentley. 1991. Correlations of soil properties. Billing and Sons, Ltd., Worcester, UK.

Chapin, F.S., III, T. Hollingsworth, D.F. Murray, L.A. Viereck, and M.D. Walker. 2006. Floristic diversity and vegetation distribution in the Alaskan boreal forest. In: F.S. Chapin, III, M.W. Oswood, K. Van Cleve, L.A. Viereck, and D.L. Verbyla, editors, Alaska's changing boreal forest. Oxford Univ. Press, Inc., New York. p. 81–99.

Clark, M.H., and D.R. Kautz. 1999. Soil survey of Copper River area, Alaska. USDA–NRCS, Washington, DC.

Collins, M., R. Knutt, J. Arblaster, J.-L. Dufresne, T. Fichefet, P. Friedlingstein, et al. 2013. Long-term climate change: Projections, commitments and irreversibility. In: T.F. Stocker, D. Qin, G.-K. Plattner, M. Tignor, S.K. Allen, J. Boschung, A. Nauels, Y. Xia, V. Bex, and P.M. Midgley, editors,

Climate change 2013: The physical science basis. Contribution of working group I to the fifth assessment report of the intergovernmental panel on climate change. Cambridge Univ. Press, Cambridge, UK and New York. p. 1029–1136.

Dimo, V.N. 1965. Formation of a humic-illuvial horizon in soils in permafrost. Sov. Soil Sci. 9:1013:1021.

Dyrness, C.T. 1982. Control of depth to permafrost and soil temperature by the forest floor in black spruce/feathermoss communities. Research Note PNW-396. USDA Forest Service, Pacific Northwest Forest and Range Exp. Stn., Portland, OR.

Ferrians, O.J. 1984. Pleistocene glacial history of the northeastern Copper River Basin, Alaska. GSA Abstracts Programs 16(5):282.

Fisher, J.P., C. Estop-Aragones, A. Thierry, D.J. Charman, S.A. Wolfe, I.P. Hartley, et al. 2016. The influence of vegetation and soil characteristics on active-layer thickness of permafrost soils in boreal forest. Glob. Change Biol. 22:3127–3140. doi:10.1111/gcb.13248

French, H., and Y. Shur. 2010. The principles of cryostratigraphy. Earth Sci. Rev. 101:190–206. doi:10.1016/j.earscirev.2010.04.002

Fryer, J.L. 2014. Fire regimes of Alaskan black spruce communities. USDA Forest Service, Rocky Mountain Research Station, Fire Sciences Laboratory. www.fs.fed.us/database/feis/fire_regimes/AK_black_spruce/all.html (accessed 7 Sept. 2019).

Gallant, A.L., E.F. Binnian, J.M. Omernik, and M.B. Shasby. 1995. Ecoregions of Alaska. USGS, DEnver, CO.

Genet, H., A.D. McGuire, K. Barrett, A. Breen, E.S. Euskirchen, J.F. Johnstone, et al. 2013. Modeling the effects of fire severity and climate warming on active layer thickness and soil carbon storage of black spruce forests across the landscape in interior Alaska. Environ. Res. Lett. 8(4):045016. doi:10.1088/1748-9326/8/4/045016

Gewehr, S., I. Drobyshev, F. Berninger, and Y. Bergeron. 2014. Soil characteristics mediate the distribution and response of boreal trees to climatic variability. Can. J. For. Res. 44(5):487–498. doi:10.1139/cjfr-2013-0481

Geophysical Institute Permafrost Laboratory, University of Alaska-Fairbanks (GIPL). 2019. Surface datasets for Gakona 1 borehole (2010-2017). https://permafrost.gi.alaska.edu/site/hp1 (accessed 1 Sept. 2019).

Grigal, D.F. 1973. Note on the hydrometer method of particle-size analysis. Soil Journal Serial Paper #8438, Univ. of Minnesota Agric. Exp. Stn., St. Paul.

Grosse, G., S. Goetz, A.D. McGuire, V.E. Romanovsky, and E.A.G. Schuur. 2016. Changing permafrost in a warming world and feedbacks to the Earth system. Environ. Res. Lett. 11(4):040201. doi:10.1088/1748-9326/11/4/040201

Harris, D., W.R. Horwath, and C. van Kessel. 2001. Acid fumigation of soils to remove carbonates prior to total organic carbon or carbon-13 isotopic analysis. Soil Sci. Soc. Am. J. 65:1853–1856. doi:10.2136/sssaj2001.1853

Hollingsworth, T.N. 2004. Quantifying variability in the Alaskan black spruce ecosystem: Linking vegetation, carbon, and fire history. Ph.D. diss., Univ. of Alaska-Fairbanks, Fairbanks.

Hollingsworth, T.N., M.D. Walker, F.S. Chapin, III, and A.L. Parsons. 2006. Scale-dependent environmental controls over species composition in Alaskan black spruce communities. Can. J. For. Res. 36(7):1781–1796. doi:10.1139/x06-061

Hoogsteen, M.J.J., E.A. Lantinga, E.J. Bakker, J.C.J. Groot, and P.A. Tottonell. 2015. Estimating soil organic carbon through loss on ignitions: Effects of ignition conditions and structural water loss. Eur. J. Soil Sci. 66(2):320–328. doi:10.1111/ejss.12224

Houle, G.P., E.S. Kane, E.S. Kasischke, C.M. Gibson, and M.R. Turetsky. 2018. Recovery of carbon pools a decade after wildfire in black spruce forests of interior Alaska: Effects of soil texture and landscape position. Can. J. For. Res. 48:1–10. doi:10.1139/cjfr-2017-0236

Hugelius, G., J. Routh, P. Kuhry, and P. Crill. 2012. Mapping the degree of decomposition and thaw remobilization potential of soil organic matter in discontinuous permafrost terrain. J. Geophys. Res. 117:G02030. doi:10.1029/2011JG001873

Hugelius, G., J. Strauss, S. Zubrzycki, J.W. Harden, E.A.G. Schuur, C.-L. Ping, et al. 2014. Estimated stocks of circumpolar permafrost carbon with quantified uncertainty ranges and identified data gaps. Biogeosciences 11:6573–6593. doi:10.5194/bg-11-6573-2014

Jafarov, E.E., S.S. Marchenko, and V.E. Romanovsky. 2012. Numerical modeling of permafrost dynamics in Alaska using a high spatial resolution dataset. Cryosphere 6:613–624. doi:10.5194/tc-6-613-2012

Jiang, Y., A.V. Rocha, J.A. O'Donnell, J.A. Drysdale, E.B. Rastetter, G.R. Shaver, and Q. Zhuang. 2015. Contrasting soil thermal responses to fire in Alaskan tundra and boreal forest. J. Geophys. Res. Earth Surf. 120:363–378. doi:10.1002/2014JF003180

Johnson, K. D., J. Harden, A.D. McGuire, N.B. Bliss, J.G. Bockheim, M. Clark, et al. 2011. Soil carbon distribution in Alaska in relation to soil-forming factors. Geoderma 167-168:71–84. doi:10.1016/j.geoderma.2011.10.006

Johnstone, J.F., T.N. Hollingsworth, and F.S. Chapin, III. 2008. A key for predicting postfire successional trajectories in black spruce stands of interior Alaska. USDA Forest Service, Pacific Northwest Research Station General Technical Report PNW-GTR-767. Pacific Northwest Forest and Range Exp. Stn., Portland, OR. doi:10.2737/PNW-GTR-767

Jorgenson, M.T., K. Yoshikawa, M. Kanevskiy, Y. Shur, V. Romanovsky, S. Marchenko, et al. 2008. Permafrost characteristics of Alaska. In: D.L. Kane and K.M. Hinkel, editors, Proceedings of the 9th International Conference on Permafrost, Institute for Northern Engineering, Univ. of Alaska-Fairbanks, Fairbanks. 29 June–3 July. p. 121–122.

Jorgenson, M.T., V. Romanovsky, J. Harden, Y. Shur, J. O'Donnell, E.A.G. Schuur, et al. 2010. Resilience and vulnerability of permafrost to climate change. Can. J. For. Res. 40(7):1219–1236. doi:10.1139/X10-060

Kasischke, E.S., and M.R. Turetsky. 2006. Recent changes in the fire regime across the North American boreal region- spatial and temporal patterns of burning across Canada and Alaska. Geophys. Res. Lett. 33:L09703.

Kasischke, E.S., D.L. Verbyla, T.S. Rupp, A.D. McGuire, K.A. Murphy, R. Jandt, et al. 2010. Alaska's changing fire regime: Implications for the vulnerability of its boreal forests. Can. J. For. Res. 40(7):1313–1324. doi: 10.1139/X10-098

Kaverin, D. 2008. Study of the transient layer developed in permafrost-affected soils of southern tundra (European North-East of Russia). 5th Northern Research Forum–Plenary Session II: The new geography of a warming north. 24–27 September. Univ. of Alaska-Anchorage, Anchorage.

Konert, M., and J. Vandenberghe. 1997. Comparison of laser grain size analysis with pipette and sieve analysis: A solution for the underestimation of the clay fraction. Sedimentology 44:523–535. doi:10.1046/j.1365-3091.1997.d01-38.x

Koven, C., P. Friedlingstein, P. Cais, D. Khvorostyanov, G. Krinner, and C. Tarnocai. 2009. On the formation of high-latitude carbon stocks: Effects of cryoturbation and insulation by organic matter in a land surface model. Geophys. Res. Lett. 36:L21501. doi:10.1029/2009GL040150

LANDFIRE. 2017. LANDFIRE biophysical settings layer: LF 2014– LF 1.4.0. US Department of Interior, Geological Survey. www.landfire.gov/lf_140.php (accessed 29 Mar. 2019).

Lerbekmo, J.F. 2008. The White River ash: Largest Holocene Plinian tephra. Can. J. Earth Sci. 45:693–700. doi:10.1139/E08-023

Lynch, J.A., J.L. Hollis, and F.S. Hu. 2004. Climatic and landscape controls of the boreal forest fire regime: Holocene records from Alaska. J. Ecol. 92(3):477–489. doi:10.1111/j.0022-0477.2004.00879.x

McCray, J.M., A.L. Wright, Y. Luo, and S. Ji. 2012. Soil phosphorus forms related to extractable phosphorus in the Everglades Agricultural Area. Soil Sci. 177(1):31–38. doi:10.1097/SS.0b013e31823782da

Michaelson, G.J., C.L. Ping, and J.M. Kimble. 1996. Carbon content and distribution in tundra soils in arctic Alaska, U.S.A. Arct. Alp. Res. 28:414–424. doi:10.2307/1551852

Michaelson, G.J., C.-L. Ping, and M. Clark. 2013. Soil pedon carbon and nitrogen data for Alaska: An analysis and update. Open J. Soil Sci. 3(2):132–142. doi:10.4236/ojss.2013.32015

Miller, B.A., and R.J. Schaetzl. 2012. Precision of soil particle size analysis using laser diffractometry. Soil Sci. Soc. Am. J. 76:1719–1727. doi:10.2136/sssaj2011.0303

Minsley, B.J., N.J. Pastick, B.K. Wylie, D.R.N. Brown, and M. Kass. 2016. Evidence for nonuniform permafrost degradation after fire in boreal landscapes. J. Geophys. Res. Earth Surf. 121:320–335. doi:10.1002/2015JF003781

Mishra, U., J.D. Jastrow, R. Matamala, G. Hugelius, C.D. Koven, J.W. Harden, et al. 2013. Empirical estimates to reduce modeling uncertainties of soil organic carbon in permafrost regions: A review of recent progress and remaining challenges. Environ. Res. Lett. 8(3):035020. doi:10.1088/1748-9326/8/3/035020

Muhs, D.R., J.R. Budahn, J.P. McGeehin, E.A. Bettis, G. Skipp, J.B. Paces, and E.A. Wheeler. 2013. Loess origin, transport, and deposition over the past 10,000 years, Wrangell-St. Elias National Park, Alaska. Aeolian Res. 11:85–99. doi:10.1016/j.aeolia.2013.06.001

Murton, J.B., and H.M. French. 1994. Cryostructures in permafrost, Tuktoyaktuk coastlands, western arctic Canada. Can. J. Earth Sci. 31(4):737–747.

doi:10.1139/e94-067
Nelson, F.E., O.A. Anisimov, and N.I. Shiklomanov. 2001. Subsidence risk from thawing permafrost. Nature 410:889–890. doi:10.1038/35073746
Nowacki, G., P. Spencer, M. Fleming, T. Brock, and M.T. Jorgenson. 2001. Ecoregions of Alaska. Open-File Report 02-297 [map]. USGS, Reston, VA. https://pubs.er.usgs.gov/publication/ofr2002297 (accessed 7 Sept. 2019). doi:10.3133/ofr2002297
O'Donnell, J.A., V.E. Romanovsky, J.W. Harden, and A.D. McGuire. 2009. The effect of moisture content on the thermal conductivity of moss and organic soil horizons from black spruce ecosystems in interior Alaska. Soil Sci. 174(12):646–651. doi:10.1097/SS.0b013e3181c4a7f8
O'Donnell, J.A. 2010. The effects of permafrost degradation on soil carbon in Alaska's boreal region. Ph.D. diss., Univ. of Alaska-Fairbanks.
O'Donnell, J.A., J.W. Harden, A.D. McGuire, M.Z. Kanevskiy, M.T. Jorsenson, and X.O. Xu. 2011. The effect of fire and permafrost interactions on soil carbon accumulation in an upland black spruce ecosystem of interior Alaska: Implications for post-thaw carbon loss. Glob. Change Biol. 17:1461–1474. doi:10.1111/j.1365-2486.2010.02358.x
Palmtag, J., and P. Kuhry. 2018. Grain size controls on cryoturbation and soil organic carbon density in permafrost-affected soils. Permafr. Periglac. Process. 29:112–120. doi:10.1002/ppp.1975
Pastick, N.J., M.T. Jorgenson, B.K. Wylie, S.J. Nield, K.D. Johnson, and A.O. Finley. 2015. Distribution of near-surface permafrost in Alaska: Estimates of present and future conditions. Remote Sens. Environ. 168:301–315. doi:10.1016/j.rse.2015.07.019
Pastick, N.J., P. Duffy, H. Genet, T.S. Rupp, B.K. Wylie, K.D. Johnson, et al. 2017. Historical and projected trends in landscape drivers affecting carbon dynamics in Alaska. Ecol. Appl. 27(5):1383–1402. doi:10.1002/eap.1538
Pastick, N.J., M.T. Jorgenson, S.J. Goetz, B.M. Jones, B.K. Wylie, B.J. Minsley, et al. 2019. Spatiotemporal remote sensing of ecosystem change and causation across Alaska. Glob. Change Biol. 25:1171–1189. doi:10.1111/gcb.14279
Ping, C.-L., M.H. Clark, and D.K. Swanson. 2004. Cryosols in Alaska. In: J.M. Kimble, editor, Cryosols. Springer-Verlag, Heidelberg, Germany. p. 71–94 doi:10.1007/978-3-662-06429-0_5
Ping, C.-L., G.J. Michaelson, J.M. Kimble, V.E. Romanovsky, Y.L. Shur, D.K. Swanson, and D.A. Walker. 2008. Cryogenesis and soil formation along a bioclimate gradient in Arctic North America. J. Geophys. Res. 113:G03S12. doi:10.1029/2008JG000744
Ping, C.-L., G.J. Michaelson, E.S. Kane, E.C. Packee, C.A. Stiles, D.K. Swanson, and N.D. Zaman. 2010. Carbon stores and biogeochemical properties of soils under black spruce forest, Alaska. Soil Sci. Soc. Am. J. 74(3):969–978. doi:10.2136/sssaj2009.0152
Ping, C.L., M.H. Clark, J.M. Kimble, G.J. Michaelson, Y. Shur, and C.A. Stiles. 2013. Sampling protocols for permafrost-affected soils. Soil Horiz. 54(1):13–19. doi:10.2136/sh12-09-0027
Ping, C.-L., J.D. Jastrow, M.T. Jorgenson, G.J. Michaelson, and Y.L. Shur. 2015. Permafrost soils and carbon cycling. Soil (Gottingen) 1:147–171. doi:10.5194/soil-1-147-2015
Potter, C., and C. Hugny. 2018. Wildfire effects on permafrost and soil moisture in spruce forests of interior Alaska. J. For. Res. doi:10.1007/s11676-018-0831-2
Preece, S.J., R.G. McGimsey, J.A. Westgate, N.J.G. Pearce, W.K. Hart, and W.T. Perkins. 2014. Chemical complexity and source of the White River Ash, Alaska and Yukon. Geosphere 10(5):1020–1042. doi:10.1130/GES00953.1
R Core Team. 2016. R: A language and environment for statistical computing. R Foundation for Statistical Computing, Vienna, Austria.
Rand, J., and M. Mellor. 1985. Ice-coring augers for shallow depth sampling. CRREL Report 85-21. U.S. Army Corps of Engineers Cold Regions Research & Engineering Laboratory, Hanover, NH. https://apps.dtic.mil/dtic/tr/fulltext/u2/a166630.pdf (accessed 7 Sept. 2019).
Reiger, S. 1983. The genesis and classification of cold soils. Academic Press, Inc., New York.
Riehle, J.R., P.M. Bowers, and T.A. Ager. 1990. The Hayes tephra deposits, and upper Holocene marker horizon in south-central Alaska. Quat. Res. 33(3):276–290. doi:10.1016/0033-5894(90)90056-Q
Rubin, M., and C. Alexander. 1960. U.S. Geological Survey radiocarbon dates V. Radiocarbon 2:129–185.
Schoeneberger, P.J., D.A. Wysocki, and E.C. Benham, and Soil Survey Staff. 2012. Field book for describing and sampling soils, version 3.0. USDA–NRCS National Soil Survey Center, Lincoln, NE.
Schwarz, G. 1978. Estimating the dimension of a model. Ann. Stat. 6:461–464. doi:10.1214/aos/1176344136
Shur, Y., K.M. Hinkel, and F.E. Nelson. 2005. The transient layer: Implications for geocryology and climate-change science. Permafr. Periglac. Process. 16:5–17. doi:10.1002/ppp.518
Shur, Y., and M.T. Jorgenson. 2007. Patterns of permafrost formation and degradation in relation to climate and ecosystems. Permafr. Periglac. Process. 18:7–19. doi:10.1002/ppp.582
Shur, Y., T. Jorgenson, M. Kanevskiy, and C.-L. Ping. 2008. Formation of frost boils and earth hummocks. In: D.L. Kane and K.M. Hinkel, editors, Proceedings of the 9th International Conference on Permafrost, Institute for Northern Engineering, Univ. of Alaska-Fairbanks, Fairbanks. 29 June–3 July. CRC Press, Boca Raton, FL. p. 287–288.
Shur, Y., and T. Zhestkova. 2003. Cryogenic structure of a glacio-lacustrine deposit. In: W. Haeberli, and D. Brandova, editors, Proceedings of the 8th International Conference on Permafrost, Zurich, Switzerland. CRC Press, Boca Raton, FL. 20–25 July. p. 1051–1056.
Soil Survey Staff. 2014a. Kellogg soil survey laboratory methods manual. R. Burt and Soil Survey Staff, editors, Soil survey investigations report no. 42, version 5.0. USDA–NRCS, Washington, DC.
Soil Survey Staff. 2014b. Keys to soil taxonomy, 12th ed. USDA–NRCS, Washington, DC.
Spiess, A.N., and N. Neumeyer. 2010. An evaluation of R^2 as an inadequate measure for nonlinear models in pharmacological and biochemical research: A Monte Carlo approach. BMC Pharmacol. 10:6. doi:10.1186/1471-2210-10-6
Swanson, D.K., C.L. Ping, and G.J. Michaelson. 1999. Diapirism in soils due to thaw of ice-rich material near the permafrost table. Permafr. Periglac. Process. 10:349–367. doi:10.1002/(SICI)1099-1530(199910/12)10:4<349::AID-PPP318>3.0.CO;2-N
Vasil'chuk, Y.K., S.V. Alekseev, S.G. Arzhannikov, L.P. Alekseeva, N.A. Budantseva, N. Chizhova Ju, et al. 2015. Oxygen and hydrogen isotope compositions of lithalsa frozen core: A case study from the Sentsa River Valley, East Sayan. Kriosfera Zemli XIX(2):46–58.
Viereck, L.A., and C.T. Dyrness, editors. 1979. Ecological effects of the Wickersham Dome fire near Fairbanks, Alaska. USDA Forest Service, Pacific Northwest Research Station Gen. Tech. Rep. PNW-90. Pacific Northwest Forest and Range Experiment Station, Portland, OR.
Viereck, L.A., K. Van Cleve, and C.T. Dyrness. 1986. Forest ecosystem distribution in the taiga environment. In: K. Van Cleve, F.S. Chapin, III, P.W. Flanagan, L.A. Viereck, and C.T. Dyrness, editors, Forest ecosystems in the Alaskan taiga: A synthesis of structure and function. Ecological Studies 57. Springer-Verlag, New York. p. 22–43. doi:10.1007/978-1-4612-4902-3_3
Weast, R.C. 1981. Handbook of chemistry and physics. 61st ed. CRC Press, Boca Raton, FL.
Webb, E.E., K. Heard, S.M. Natali, A.G. Bunn, H.D. Alexander, L.T. Berner, et al. 2017. Variability in above- and belowground carbon stocks in a Siberian larch watershed. Biogeosciences 14:4279–4294. doi:10.5194/bg-14-4279-2017
Wiedmer, M., D.R. Montgomery, A.R. Gillespie, and H. Greenberg. 2010. Late quaternary megafloods from Glacial Lake Atna, southcentral Alaska, U.S.A. Quaternary Res. 73:413–424.
Williams, J.R., and J.P. Galloway. 1986. Map of western Copper River Basin, Alaska showing lake sediments and shorelines, glacial moraines, and location of stratigraphic sections and radiocarbon-dated samples. Open-File Report 86-390. USGS, Reston, VA.
Wright, A.L., Y. Wang, and K.R. Reddy. 2008. Loss-on-ignition method to assess soil organic carbon in calcareous Everglades wetlands. Commun. Soil Sci. Plant Anal. 39:3074–3083. doi:10.1080/00103620802432931
Yarie, J., and S. Billings. 2002. Carbon balance of the taiga forest within Alaska: Present and future. Can. J. For. Res. 32(5):757–767. doi:10.1139/x01-075
Yoshikawa, K., W.R. Bolton, V.E. Romanovsky, M. Fukuda, and L.D. Hinzman. 2003. Impacts of wildfire on the permafrost in the boreal forests of interior Alaska. J. Geophys. Res. 108(D1):8148. doi:10.1029/2001JD000438